OPEN ACCESS

geosciences

Article

Mesozoic–Cenozoic Evolution of the Western Margin of South America: Case Study of the Peruvian Andes

O. Adrian Pfiffner * and Laura Gonzalez

Institute of Geological Sciences, University of Bern, Baltzerstrasse 1+3, Bern CH3012, Switzerland;
E-Mail: laura.gonzalez@geo.unibe.ch

* Author to whom correspondence should be addressed; E-Mail: adrian.pfiffner@geo.unibe.ch;
Tel.: +41-31-631-8757; Fax: +41-31-631-4843.

Abstract: Based on the structural style and physiographic criteria, the Central Andes of Peru can be divided into segments running parallel to the Pacific coast. The westernmost segment, the Coastal Belt, consists of a Late Jurassic–Cretaceous volcanic arc sequence that was accreted to the South American craton in Cretaceous times. The Mesozoic strata of the adjacent Western Cordillera represent an ENE-vergent fold-and-thrust belt that formed in Eocene times. Tight upright folds developed above a shallow detachment horizon in the West, while more open folds formed above a deeper detachment horizon towards the East and in the neighboring Central Highlands. A completely different style with steeply dipping reverse faults and open folds affecting the Neoproterozoic crystalline basement is typical for the Eastern Cordillera. The Subandean Zone is characterized by mainly NE-vergent imbricate thrusting which occurred in Neogene times. A quantitative estimate of the shortening of the orogen obtained from balanced cross-sections indicates a total shortening of 120–150 km (24%–27%). This shortening was coeval with the Neogene westward drift of South America, occurred at rates between 3 and 4.7 mm/year and was responsible for the high elevation of the Peruvian Andes.

1. Introduction

The Andean chain straddles the western coast of the South American continent, parallel to a subduction zone where the Nazca plate descends beneath the South American continental plate (Figure 1). The geometry of the subducting Nazca plate varies along this Peru–Chile trench. Beneath Ecuador, southern Peru, northern and southern Chile the angle of subduction is between 25° and 30°, and these regions are characterized by active volcanism. In the segments of northern and central Peru, as well as central Chile, the Nazca plate descends at shallow angles to a depth of 100 km with little or no asthenospheric mantle between the plates. As a consequence these regions lack volcanic activity [1–6].

Figure 1. Topographic overview map of South America showing the distribution of volcanoes within the Andes, the plate boundary, the ridges within the Pacific Ocean and the study area in the Central Andes of Peru.

The structure of the Andes themselves also undergoes significant changes along strike. The Northern Andes, including the segment of Ecuador just north of our study area, involved the accretion of oceanic terranes to the South American Plate in Cretaceous to Paleocene times [3]. The Central Andes are dominated by the subduction of oceanic crust and the Southern Andes formed in response to

uplift caused by ridge collisions [3]. Within the Central Andes, the lack of volcanic activity in the Peruvian segment in the last 10 Ma and the deep incision by the rivers draining the western flank of the mountain range exposed the fold-and-thrust structures in the Mesozoic sedimentary sequences. In contrast, in the adjacent segment to the south, thick volcanic deposits dominate and prohibit a direct observation of the structures underneath. It was for this reason that the Central Andes of Peru were chosen as study area.

In the Central Andes of Peru, the crustal deformation of the South American plate has produced three main geomorphic features differing in structural style. Two cordilleras, the Western and Eastern Cordillera, run parallel to the coast and are separated by an intermontane plateau, the Central Highlands. The general topography is shown in Figure 2 in form of a simple digital elevation model (adapted from [7]). The cordilleras of the Central Andes possess a rugged relief with peaks reaching elevations of more than 6000 m. A more gentle relief is present in the central part of Peru, in the Central Highlands. Here, the mean elevation is about 4000 m.

Figure 3 shows a general cross-section through the plate boundary. The Nazca plate dipping beneath the South American plate has a flat segment at less than 120 km depth beneath much of the Andes [1,3–5]. Farther inland, it dips to the northeast beneath the Amazonas Craton. Much of the flat slab is most likely composed of an oceanic plateau associated with the Nazca Ridge. Assuming a symmetric spreading geometry along the Pacific spreading ridge, this plateau is an equivalent to the Tuamotu Plateau now present east of Tsonga. The thick oceanic crust of this plateau may well be responsible for the shallow dip of the Nazca plate in this cross-section. The crustal structure of the South American Plate in Figure 3 is based on [8–11] and shows a 60 km deep crustal root beneath the Western Cordillera. Towards the Amazonas Craton the crust-mantle boundary is at a depth of 35 km. As shown by the 3D-model of [9], the geometry of the plate boundary and the crustal structure undergo important changes going southeast along strike of the Andes.

The Proto-Andean margin was the site of continental accretion in the course of the Neoproterozoic and Paleozoic [12–14]. Here we concentrate on the Mesozoic to Cenozoic evolution, which includes the accretion or amalgamation of the Casma Volcanic Arc to the South American continent in the Cretaceous. This arc is composed of a volcaniclastic sequence that overlies a Proterozoic–Early Paleozoic complex of high-grade metamorphic rocks and granites (Arequipa Massif). The accretion corresponds to the emplacement of a crustal block along an NE-vergent thrust fault with moderate internal deformation of the accreted block. Although the accretion occurred in the framework of oblique plate convergence, the lateral displacement of the accreted block was minor [15].

The structural evolution of the Peruvian Andes has been described as a sequence of regionally recognized phases of deformation. These phases were interpreted as a deformation front migrating eastward from the Pacific coast to the Subandean Zone [16–20]. In the Western Cordillera, Early Cretaceous plutons of the Coastal Batholith intruded folded Jurassic to Early Cretaceous volcaniclastics, indicating a phase of shortening in the Early Cretaceous which has been referred to as *Mochica* phase in the literature [19,21]. The latest Cretaceous to Early Paleocene strata of the Casapalca Formation within the Marañon fold-and-thrust belt are continental deposits [17,18,20,22]. The change from marine sedimentation of the Jurassic and Early Cretaceous to continental sedimentation in the Late Cretaceous suggests an uplift, which is suspected to be caused by a phase of compression (op. cit.) and designated as *Peruvian* phase. The development of the Marañon fold-and-thrust belt in the Western

Cordillera is attributed to a major phase of deformation, the *Incaic* phase, that has been documented as Mid to Late Eocene in age. The phase is bracketed by an unconformity between the Mid Eocene to Early Miocene volcanics of the Calipuy Group (and equivalents) and the eroded upright folds in the Marañon fold-and-thrust belt [17–20]. Evidence for a Neogene phase of deformation, referred to as *Quechua* phase, have been recognized within the Subandean thrust belt in the eastern foothills of the Eastern Cordillera where Miocene and Pliocene clastics are affected by thrust faults [18,22,23]. As will be discussed later, the overall spatial and temporal distribution of deformation in the study area is more complex than a simple migrating deformation front.

Figure 2. Digital elevation map of the Central Andes based on [7] showing the main geomorphic features. Peaks exceeding elevations of 5000 m are aligned along the Western and the Eastern Cordilleras. The Central Highlands pinch out towards the NNW and widen towards the Altiplano in the SE.
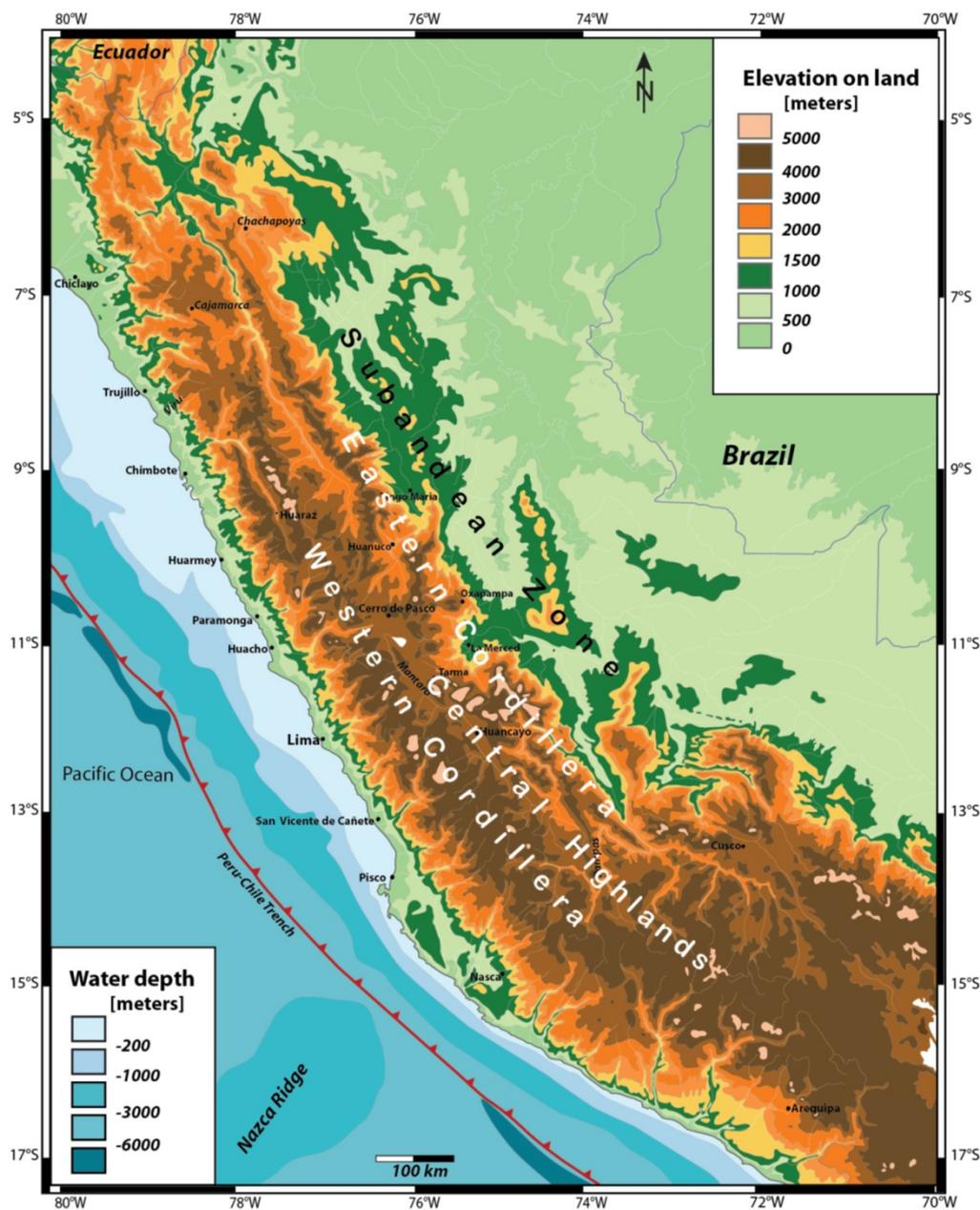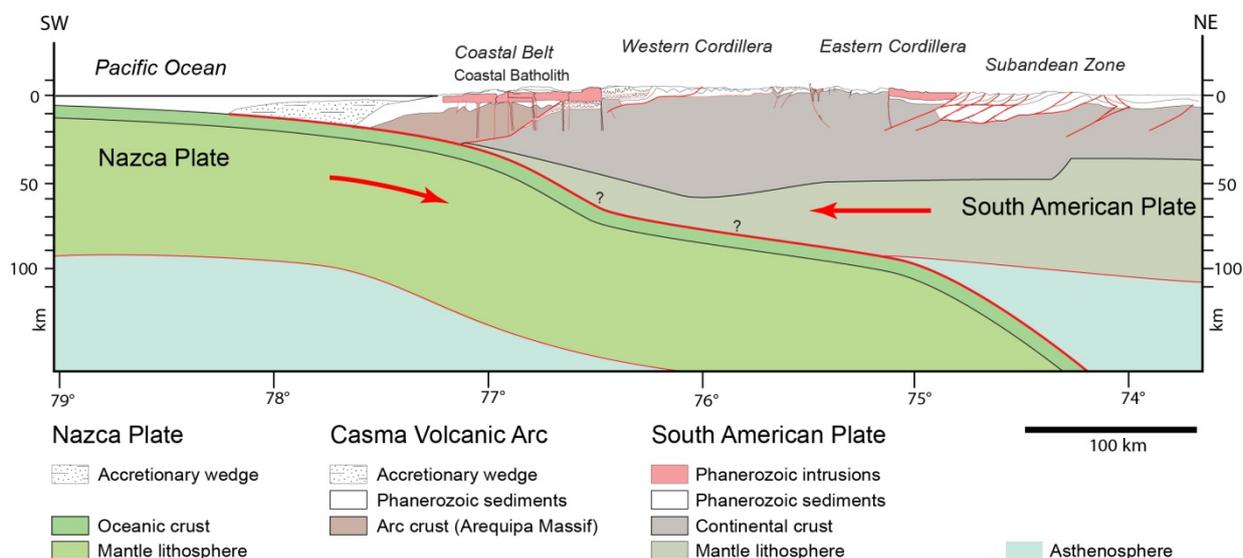
Figure 3. General cross-section showing the geometry of the plate boundary in the subduction zone and the crustal structure of the Andes [8–11]. Upper crustal structure of the Andes after own work.


The absence of recent volcanism and the steep gorges and high local relief that the rivers have created along their courses make the Central Peruvian Andes a magnificent place to analyze the structural style and evolution of this well exposed mountain belt. Although the structural style of the Peruvian Andes and the evolution of this mountain belt have been described by earlier workers [17–19] and summarized in [20], a complete structural model for the Central Peruvian Andes based on modern tools of structural geology and combined with geophysical data is still lacking.

The aim of this paper is to develop such a structural model and to put it into the framework of the kinematic evolution of the orogen. It includes a discussion of the Paleozoic–Cenozoic sedimentary succession and the contemporary magmatism. The structural model is constrained with the compilation of a structural map of the orogen and the construction of two balanced cross-sections across the entire orogen. The cross-sections are intended to give a holistic view of the entire orogen including structural style, geometric relationships between plutonic and volcanic rocks, age distribution of sedimentary sequences with associated synsedimentary faults, as well as the plate geometry based on geophysical data. A series of local cross-sections demonstrates field arguments used for building a model for the evolution of the orogeny.

2. Stratigraphy

In the Central Peruvian Andes, the Phanerozoic successions of the Coastal Belt, the Cordilleras, the Central Highlands and the Subandean Zone differ considerably. Figure 4 shows the variation in stratigraphy within these areas. The stratigraphic sections are compiled from published sections and from our own field observations. The crystalline basement rocks crop out in the Eastern Cordillera mainly and have been grouped into the Marañon Complex in the north and the Huaytapallana Massif in the central part following [17] and [24]. These units comprise Neoproterozoic to Early Paleozoic high-grade orthogneisses and metasedimentary sequences [12,25]. A number of smaller outcrops of crystalline basement crop out in the Coastal Belt in the area of Arequipa and are grouped into the Arequipa Massif.

Figure 4. Stratigraphic framework of the Central Andes. The stratigraphic sequences and lateral variations are displayed by means of a set of carefully selected typical columns. See text for discussion and references used for this compilation. An enlarged version of this figure is available in the supplementary material (Figure S1).
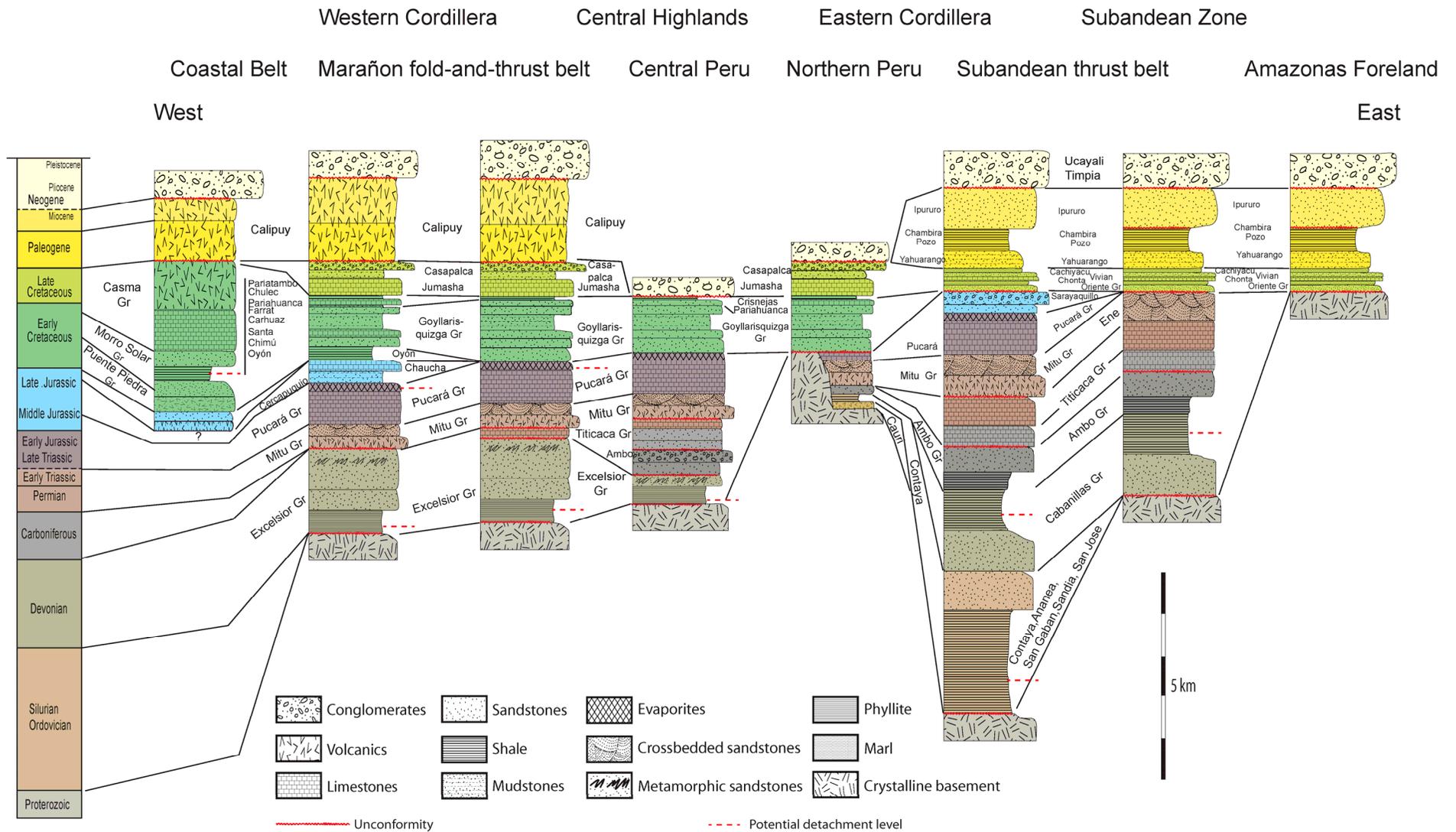
2.1. Western Cordillera

2.1.1. Coastal Belt

Outcrops of crystalline basement in the Arequipa Massif include high-grade, partly migmatized gneisses and schists that are intruded by Early Paleozoic granites [15].

The sediments of the Coastal Belt are of Jurassic (Tithonian) and Cretaceous age and represent a 5000 m thick volcanic arc sequence (see Figure 4). At the base, the Puente Piedra Group contains a volcaniclastic sequence comprising basaltic to andesitic lava flows, shales and subordinate limestones [26–28]; the Morro Solar and the Imperial Groups are clastic in nature with shaly-sandy and carbonate units [29]. The highest unit, the Casma Group, records a volcanic episode in the Early Cretaceous (Albian) and consists of pillow lavas, sheet lavas and tuffs of basaltic and andesitic composition, with minor clastic sediments. According to [30], sedimentation in the Casma Group of the area around Lima prevailed up into Late Cretaceous times. The basement of this submarine volcanic arc deposits is nowhere exposed in the area [29,31,32]. The entire sequence is intruded by the Coastal Batholith and overlain by the volcanic rocks of the Calipuy Group.

2.1.2. Marañon Fold-and-Thrust Belt

The sedimentary sequences of the Marañon fold-and-thrust belt were deposited in two distinct environments, the Western and the Eastern Peruvian troughs. In the eastern trough, shallow marine and continental conditions predominated, while in the western trough subsidence was more important as indicated by the greater thicknesses of the various formations (The Devonian sediments of the Excelsior Group represent the oldest unit within the Marañon fold-and-thrust belt (Figure 4). Unmetamorphosed sandstones, black shales and phyllites unconformably overlie Devonian metamorphic schists. These Devonian sediments of the Excelsior Group are restricted to the Western Peruvian trough [33,34]. North of Cerro de Pasco, at the western border of the Eastern Cordillera, Ordovician and Silurian rocks form the base of the Paleozoic succession (see [35] and discussion below). The sediments of the Excelsior Group are overlain unconformably by Permian volcanics and cross-bedded red sandstones of the Mitu Group. The Triassic to Jurassic Pucará Group consists of limestones, dolostones, fine-grained organic rich clastics and evaporitic layers on the top [36,37]. The deep to shallow marine sediments of the Pucará group are present throughout the entire region of the Central Peruvian Andes. Fluvial sandstones of the Cercapuquio Formation and limestones, red siltstones and dolostones of the Chaucha Formation, both of Middle Jurassic age, unconformably overlie the Pucará Group [38]. These strata are outcropping in the cores of folds of the Marañon fold-and-thrust belt. Farther to the east, in the Central Highlands, the Cercapuquio and Chaucha Formation pinch out such that Cretaceous sediments come to rest directly on the Triassic–Jurassic limestone of the Pucará Group.

The Cretaceous strata were deposited in two sub-basins of the West Peruvian trough separated by a synsedimentary fault system (Chonta Fault; [35]). In the western sub-basin, the Oyón, Chimú, Santa, Carhuaz, Farrat, Parihuanca, Chulec, Pariatambo and Crisnejas formations were deposited. These units mainly consist of fluvial to deltaic clastics with sandstones, shales and some limestones [26,32,34,35,39]. The Oyón Formation contains sandstones and shales interbedded with coal layers at the base, and metaquartzites at the top. The lower part of this formation has been considered as a detachment

horizon within the Marañon fold-and-thrust belt [17,18,39]. These shales and coal beds are rapidly replaced by sandstones towards the east. The abrupt lateral facies change is linked to the Chonta fault [32] and provokes the eastward change in structural style within the Marañon fold-and-thrust belt from tight to more open folds. East of the Chonta Fault, the Early Cretaceous units are represented by the Goyllarisquizga Group, which contains thick layers of sandstones and is overlain by the fine-grain sandstones of the Parihuanca Formation (see Figure 4).

The Cretaceous (Albian–Maastrichtian) sediments display a change from marine to continental conditions. The Jumasha Formation contains limestones, calcareous sandstones, fossiliferous limestones and dolostones [26,40]. The limestones and dolostones of the Jumasha Formation form several of the high peaks in the Western Cordillera. A change to a continental depositional environment is indicated by the red sandstones and mudstones of the Casapalca Formation [26,34], which overly the limestones of the Jumasha Formation conformably.

A major angular unconformity separates the folded Casapalca Formation from the overlying Paleogene volcanics, a point that is discussed in more detail below.

2.2. Central Highlands

In the area of Huancayo and Oroya, Carboniferous sediments were deposited on sandstones of the Devonian Excelsior Group. The Carboniferous Ambo Group consists of conglomerates, sandstones, green mudstones and shales with some rhyolitic tuffs layers [41]. Elsewhere in the Central Highlands, the Ambo Group is overlain unconformably by the Carboniferous Tarma Formation of the Titicaca Group [42,43], which consists of green sandstones, shales and limestones. A complete Permian sequence is present in the Central Highlands. The Permian Copacabana Formation of the Titicaca Group is mainly composed of marine limestones that are overlain unconformably by red sandstones and volcanic sediments of the Permian Mitu Group (Figure 4).

Marine sediments of the Late Triassic to Early Jurassic Pucará Group overly the Permian sediments conformably. The sedimentary sequences of the Pucará Group and the overlying Cretaceous are similar to the ones of the Marañon fold-and-thrust belt discussed above. Despite the pinch-out of the Jurassic Cercapuquio and Chaucha Formations present in the Western Cordillera, the Cretaceous strata overly the evaporites of the Pucará Group conformably.

2.3. Eastern Cordillera

Outcrops of metamorphic crystalline basement rocks, designated as "Marañon Complex", are present in many places throughout the Eastern Cordillera. In the northern part of Peru, these rock types include Neoproterozoic orthogneisses dated at ~613 Ma that were intruded by granitoids in the Ordovician [12]. In the Late Ordovician and Silurian, between 450 and 420 Ma, the Cauri Volcanics followed by debris flows and sandstones interbedded with shales of the Contaya Formation [35,43,44] were deposited on this basement and subsequently metamorphosed [12]. A second volcaniclastic sequence was deposited in the Carboniferous (after 320 Ma) and metamorphosed at 310 Ma [12].

In central Peru, the crystalline basement of the "Marañon Complex" is overlain by Late Paleozoic (Devonian to Permian) and Triassic–Jurassic (Pucará Group) sedimentary sequences that are identical to the ones encountered in the Central Highlands discussed above. However, namely in certain parts of

northern Peru, these sequences are missing and the Cretaceous fluvial to shallow marine sediments of the Goyllarisquizga Group directly overly the crystalline basement of the Marañon Complex (Figure 4). The hiatus between the basement and the Cretaceous is attributed to the "Marañon geanticline", a long lasting paleogeographic high [17,26].

A number of Permo–Triassic batholiths intruded the Paleozoic sediments and the metamorphic units [21,45,46]. The batholiths follow the eastern flank of the entire Eastern Cordillera and point to the existence of a magmatic arc.

2.4. Subandean Zone

In the western basins of the Subandean Zone, the crystalline basement is overlain unconformably by thick strata of Ordovician to Silurian age (Figure 4). These units comprise the Contaya, Ananea, San Gaban, San Jose and Sandia formations which consist of thick black shales and sandstones at the base and massive sandstones in the upper part [23,47]. Overlying the Ordovician to Silurian sediments is the Devonian Cabanillas Formation, a succession of fluvial sandstones at the base followed by fossiliferous black shales (Figure 4). Outcrops of Paleozoic sediments are scarce in the study area and restricted to the Shira Mountains located south east of Satipo city. These deposits can be traced to the SE to the Bolivian Andes. The Late Paleozoic sediments on the other hand can be traced from the Western Cordillera all the way to the Subandean Zone.

In contrast to marine deposits in the Western Cordillera, the continental red beds of the Sarayaquillo Formation characterize the Late Jurassic of the Subandean thrust belt. The red conglomerates and sandstones of the Sarayaquillo Formation overly slightly unconformable evaporites and limestones of the Pucará Formation (Figure 4). The Cretaceous (Aptian–Albian) sediments of the Oriente Group (Cushabatay, Raya and Agua Caliente Formations) on their turn overlie the Jurassic sandstones of the Sarayaquillo Formation with an angular unconformity. The formations of the Oriente Group consist of coarse-grained massive cross-bedded sandstones interbedded with shales and were deposited in a continental environment [23,48]. The next units up, the Chonta and Vivian formations, are made up of calcareous mudstones and cross-bedded massive sandstones with layers of black shales. The top of the Cretaceous sequence, the Cachiyacu Formation, consists of sandy shales, marls and calcarenites.

Contrary to the Cenozoic volcanic sequences of the Western Cordillera, continental deposits were accumulated in the Huallaga and Ucayali basins of the Subandean Zone. These basins are part of a belt of foreland basins that extend from the Northern to the Southern Andes and are separated by major transverse zones across which important changes in subsidence rates occurred [49]. In the Central Andes of Peru, the thick Paleocene–Miocene sequences that conformably overly the Cretaceous sediments (Figure 4) are mainly conglomeratic sandstones, cross-bedded red sandstones, reddish to grayish siltstones and some horizons of limestones and green shales. These sediments are grouped in the Paleocene–Early Eocene Yahuarango Formation, the Eocene–Oligocene Pozo Formation, the Oligocene–Early Miocene Chambira Formation and the Miocene Ipururo Formation [48,50]. The Pliocene Timpia Formation [22] consists of coarse-grained conglomerates with well-rounded clasts in the size range of pebbles to boulders. The pebble spectra include quartzites, sandstones, limestones, granites and andesites. The Pleistocene Ucayali Formation, finally, contains conglomerates deposited in river valleys [48].

3. Magmatism

The Andes of Peru are famous for the Coastal Batholith, which was extensively studied by Pitcher and his group [51–53] for several years and has served as model intrusion to understand the emplacement of large plutons in the crust. However, additional magmatic events affected the Central Peruvian Andes and will be described in chronologic order. The oldest plutonic sequences are of Early Paleozoic [46,54,55] and Carboniferous age and must be regarded in the context of the evolution of the Proto-Andean margin on the edge of the Amazonas Craton (see [12] and references therein). Permo–Triassic granitic intrusions are hosted within Paleozoic sediments and the metamorphic basement of the Eastern Cordillera [24,45,56,57]. The volcanic deposits contained in the Mitu Group are most likely related to this Permo–Triassic magmatic arc [58].

An Early Cretaceous magmatic episode is recognized in the Coastal Belt. Here, thick beds of pillow lavas, sheet lavas and tuffs with a basaltic to intermediate composition occur within the Morro-Solar and Casma groups. According to geochemical data it has been inferred that the volcanics represent mantle-derived magmas that possibly formed in a back arc setting [59].

The volcaniclastics of this Casma Volcanic Arc were intruded by the Coastal Batholith in a magmatic episode lasting from the Late Cretaceous to the Early Paleogene [60,61]. The Coastal Batholith of Peru extends over 1680 km along the coast, parallel to the Andean trend and the Peru–Chile trench (Figure 5). Owing to the notorious arid climatic conditions the most impressive magmatic intrusive complex is rather well exposed. The name of the Coastal Batholith has been exclusively given for the chain of plutons at the western side of the Western Cordillera. The plutons of the Coastal Batholith intruded not only the Casma Volcanic Arc but also the deformed Cretaceous sediments of the Marañon fold-and-thrust belt in the Western Cordillera. The Coastal Batholith has been grouped into several super-units that form individual segments along the coast. The super-units shown in Figure 5 belong to the Arequipa and Lima segment [57,61,62]. The super-units correspond to individual intrusions with a certain composition and a clearly defined contact between them. Their emplacement is explained as a single magmatic pulse [62]. Each super-unit of the Coastal Batholith can have a range of rock types varying from gabbro-diorite to granite, which is taken to indicate a regular rhythm of intrusion and differentiation from basic to acid composition [62,63]. Through crystal fractionation during their upward passage, basaltic melts developed into a granodioritic to tonalitic composition [63–65]. The shallowest intrusives are in fact enriched in potassium feldspar and quartz. Isotope studies indicate that the magmas could have originated by partial melting in the mantle or in an underplated zone within the lower crust [66,67].

The high-level emplacement and shape of the Coastal Batholith has been a topic of discussion. Based on gravity profiles along three traverses across the Coastal Batholith, Haederle and Atherton [68] concluded that the intrusive body has a tabular geometry and that its average thickness, measured from the roof to the floor, is approximately 5 km. These authors also discuss the emplacement mechanism of these thin tabular plutons and reached the conclusion that downward displacement of the country rock via floor depression is the best explanation for creating the space required for the emplacement of the Coastal Batholith. This floor depression is thought to have occurred mainly by a "cantilever piston mechanism", in which the subsidence of the country rock pistons was accommodated by normal faults. These normal faults acted also as channels for rising melts. Stoping occurred in the roof of the

intrusions and explains the predominantly rectilinear shape of the intrusion contacts with the sediments of the coastal belt. Interestingly, the intrusive rocks of the Coastal Batholith show virtually no sign of internal deformation post-dating their emplacement.

Figure 5. Temporal and spatial distribution of magmatic rocks in the Central Andes. References for ages are discussed in the text. Lengths of bars reflect age uncertainties.
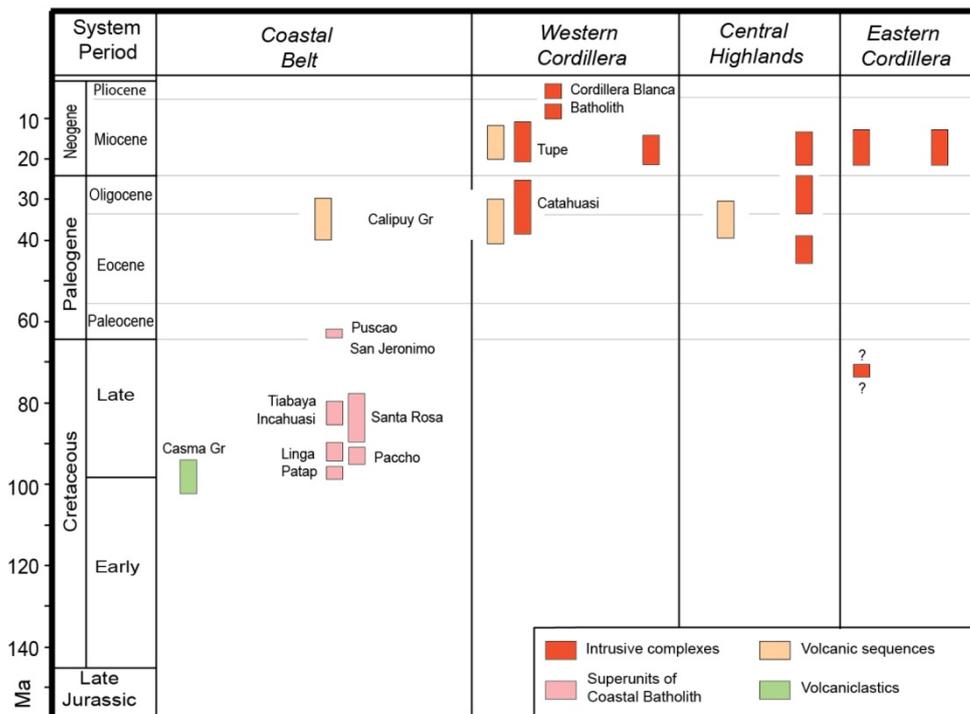
A younger magmatic episode in Eocene to Miocene times encompasses smaller batholiths that intruded the folded strata of the Marañon fold-and-thrust belt, the Central Highlands and even the western rim of the Eastern Cordillera (Figure 5; see also [69] and references therein). The Cordillera Blanca Batholith, located near Huaraz in the Northern part of the Western Cordillera (Figure 5), is the largest intrusive body of this Cenozoic magmatic arc. Cooling ages of this batholith range between 16 and 9 Ma in the tonalites and diorites, and between 6 and 2.7 Ma in the leucogranodiorite [70,71]. This intrusion now forms peaks reaching more than 6000 m. Steep faults at the western margin of the batholith (see [7], their Figure 13) raised the intrusive rocks next to the Cenozoic volcanics of the Cordillera Negra and are, combined with the low erodibility of the intrusive rocks responsible for the impressive local relief in the area.

Petrologic and isotope studies suggest that unlike the mantle-derived magmas of the Coastal Batholith, the Cenozoic intrusions had their magma source primary from partial melting in the lower crust thickened by crustal underplating [71,72]. The intrusive rocks of Cenozoic stocks present in the Cordilleras and the Central Highlands show hardly or no sign of internal deformation.

The last magmatic event is represented by Cenozoic andesitic lava flows, tuffs and ash flows that were deposited primarily in the Western Cordillera. In some localities of the Central Highlands, this event is coeval with Cenozoic intrusions. The radiometric ages of the volcanic rocks, which pertain to the Calipuy Group and equivalents, are Late Eocene to Miocene and Oligocene to Miocene [59,73,74]

as shown in Figure 5. These volcanic rocks rest unconformably on the volcaniclastic deposits of the Coastal belt, the Coastal Batholith as well as the folded and partly eroded Cretaceous sediments of the Marañon fold-and-thrust belt. The Calipuy Group has been modestly deformed only or, as observed near the coast, completely undeformed. A slight angular unconformity may be observed at the base of the Miocene basalts in the Central Highlands near Cerro de Pasco [73,75,76].

Overall, the temporal and spatial distribution of magmatism shown in Figure 5 is very similar to the one observed in the Central Andes of Chile and Bolivia farther south [77]. For the Peruvian Andes, several authors have analyzed the relationship between the age of magmatic pulses and the concurrent relative plate motion between the South American and the Nazca plates. [62] came to the conclusion that the earliest phase of magmatism (Casma Group volcanism) occurred in an extensional tectonic environment and that the ensuing granitic intrusions represent phases of compressional tectonics. [19,21] suggest that periods of high convergence rate between the two plates correlate to enhanced magmatic activity; they acknowledged a notable exception to this rule for the emplacement of the Coastal Batholith between 75 and 59 Ma, a period with a low convergence rate. [20] followed this idea and correlate the eastward shift of the magmatic arc in the Late Cretaceous (late Campanian) to a phase of uplift in Western Cordillera (the Peruvian Phase) and the eastward shift of magmatism in Eocene times to a widening of the melting zone in the asthenosphere caused by a more shallow dip of the Benioff zone. As will be discussed below in more detail, we find that the magmatic pulses are not directly linked to compressional deformation events.

4. Geological Structure

The deformation style of the Peruvian Andes is the product of compression and transpression resulting from the convergence of the Nazca Plate and the western margin of the South American Plate, and includes the accretion of an island arc. The western margin of the South American Plate was hosting marginal basins where marine and continental conditions varied in time and space. The mechanical behavior of all these units upon compression was controlled by the original basin geometries. As a result, the present day structure of the Andes varies across and along the mountain chain and reflects the paleogeographic setting to a large extent. A particularly useful proxy in this regard is the style of folds recognized across the Andes, a point that will be discussed in more detail in the following sections. These folds are usually associated with NE-vergent thrust faults. In this context it is interesting to note that this shear sense is opposite to the subduction of the Nazca Plate beneath the South American Plate.

The structural style in the Central Andes of Peru varies significantly from the island arc sequence at the Pacific coast across the deformed marginal basins in the interior of the chain to the Amazonas foreland basin. Individual segments of the orogen were analyzed in detail by a number of workers ([22,33,78,79] to name a few), while [17,18] presented a more comprehensive study. Based on these data and the 1:100,000 scale geological maps of INGEMMET, a structural map was compiled. This map, shown in Figure 6, displays the major faults along with the most important lithotypes.

Along the Pacific coast, one recognizes the gently folded Jurassic to Early Cretaceous volcaniclastics of the accreted Casma Volcanic Arc (Morro Solar, Imperial and Casma groups; [29–32]. These folded volcaniclastics will be referred to in this work as *Coastal Belt*. They were intruded by several plutons

in Late Cretaceous times. These plutons form the Coastal Batholith, which is exposed along the entire coast of Peru [52,61]. The granitic rocks within the Coastal Batholith display in most cases no deformation.

Figure 6. Structural map of the Central Andes showing the main lithotypes and faults. The map is based on local maps by [17,18,22,33,78,79], by the 1:100,000 maps of INGEMMET and own field work.
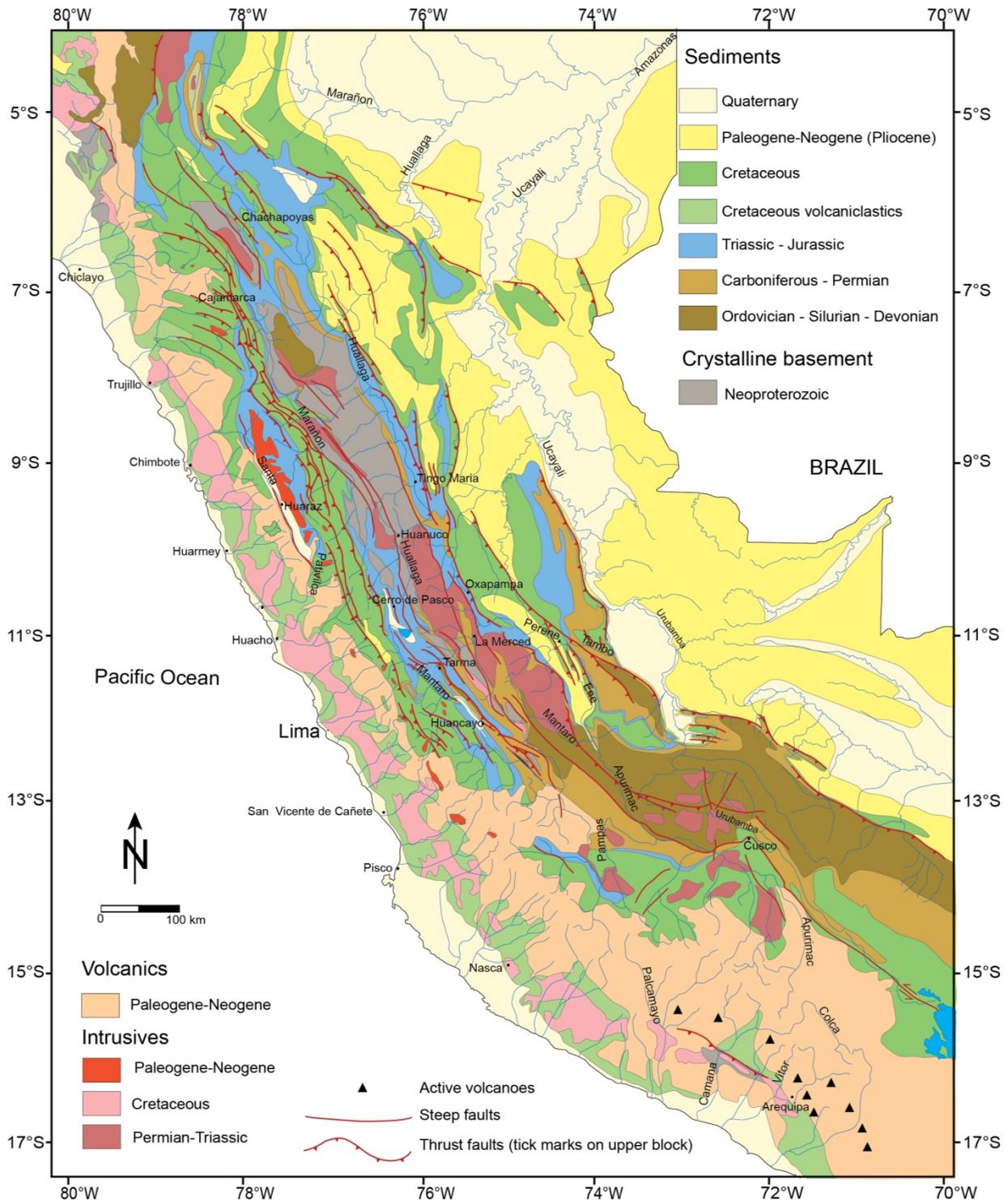
The courses of the rivers draining the *Western Cordillera* are almost straight at its western escarpment, flow within narrow deep canyons and thereby provide excellent exposure folds and faults.

Active incision of these rivers explains they flow on bare rock [7]. In the core of the Western Cordillera, Jurassic and Cretaceous strata [80] are folded and faulted [17,18,26] and form a narrow thrust belt, the so-called Marañon fold-and-thrust belt. Eocene and Miocene volcanic rocks of the Calipuy group and equivalents overlie unconformably the folded and partly eroded coastal units (Casma Group) as well as the Marañon fold-and-thrust belt [73,75].

In the *Central Highlands*, folded and faulted unmetamorphosd Paleozoic [17,43,81] and Triassic to Jurassic (Pucará Group) [36,37] sedimentary sequences are exposed. They are punctured or underlain by Permo–Triassic intrusives.

In the *Eastern Cordillera* the Neoproterozoic–Paleozoic crystalline basement is exposed. This basement referred to as Marañon Complex or Marañon "geanticline" [12–14,33,54] is affected by vertical faults in the eastern part of the Eastern Cordillera. Near Huancayo, the Huaytapallana fault system uplifted this basement next to the Paleozoic sediments. This fault system is seismically active [4,82,83]. The Paleozoic and Mesozoic strata overlying the crystalline basement are affected by large-scale folding and thrusting.

Still farther to the east, the thrust belt of the *Subandean Zone* forms the eastern foothills of the Eastern Cordillera. Paleozoic, Mesozoic and Cenozoic strata are involved in this imbricate thrust belt. Thrust faulting affected the underlying crystalline basement as well [2,22,47,50].

Late Eocene to Pleistocene magmatism is present throughout the Western and Eastern Cordillera [21,69,72,84] as witnessed by several large intrusive bodies and small plugs that cut the various fold structures.

4.1. Structural Style in Cross-Sectional View

In the following we present our analysis of the structural style, which is a prerequisite for the construction of balanced sections as presented in Section 4.2. We discuss the various structural domains individually, from the Pacific coast to the Amazonas Foreland. The analysis is based on structures including thrust faults and folds, their attitude and vergence, as well as angular unconformities. The structural styles are presented as cross-sections. The deeply incised valleys in the cordilleras are particularly useful for this type of analysis. The traces of the various cross sections are given in Figure 7.

4.1.1. Coastal Belt

The Coastal Belt displays open folds with relatively straight limbs. The fold axes are parallel to the coast. Locally, steep faults mark the hinges of folds. The folded volcaniclastic sequences are intruded by the Coastal Batholith and numerous dykes associated with it.

Structural observations at the contact clearly reveal that folding occurred prior to the intrusion, and that the granitic rocks of the intrusions reveal no sign of internal deformation.As evident on Figure 6, the Coastal Batholith runs parallel to the coast (or the Peru–Chile trench) and thus also parallel to the fold axes within the volcaniclastic country rocks. Figure 8 displays the structural style as seen along the Rio Cañete valley. The Late Cretaceous Tiabaya pluton clearly cuts the steep limb of the Early Cretaceous volcaniclastics. The latter form open folds cut by dykes (including a sill). The photograph in Figure 8B shows an example of a texture in a diorite of the Coastal Batholith that lacks any sign of deformation.

Figure 7. Structural map of the Central Andes of Peru showing traces of cross-sections. Numbers along traces correspond to figure numbers.
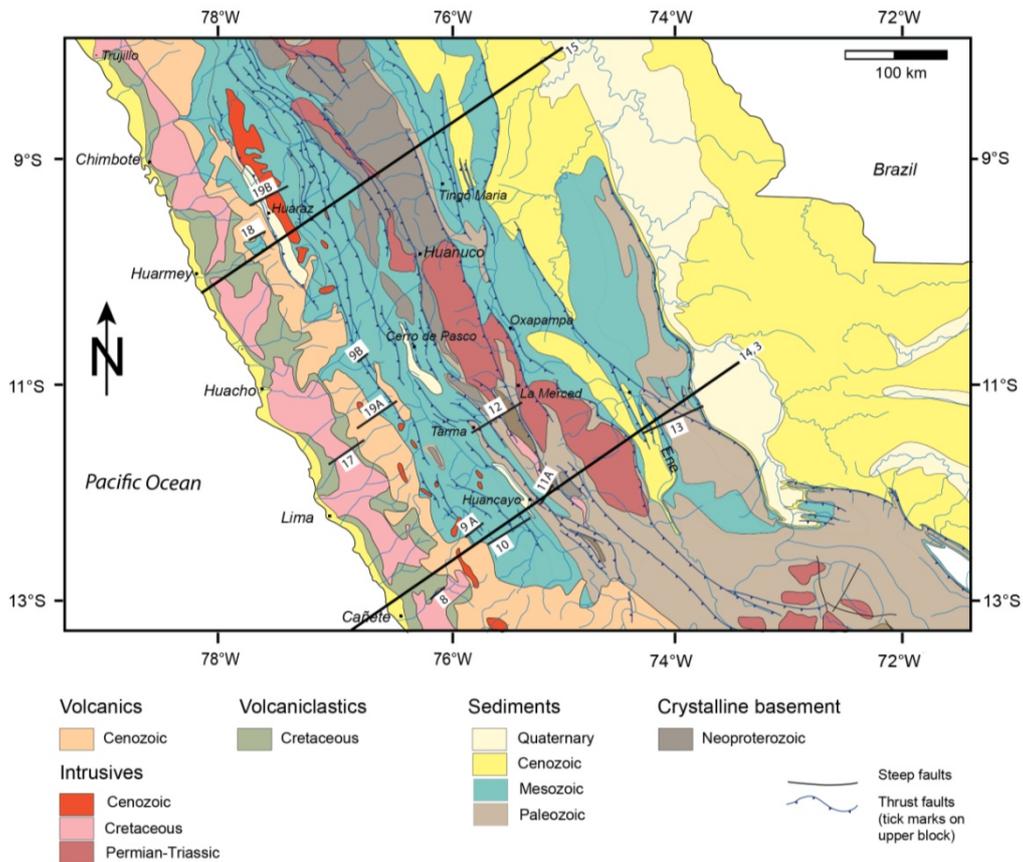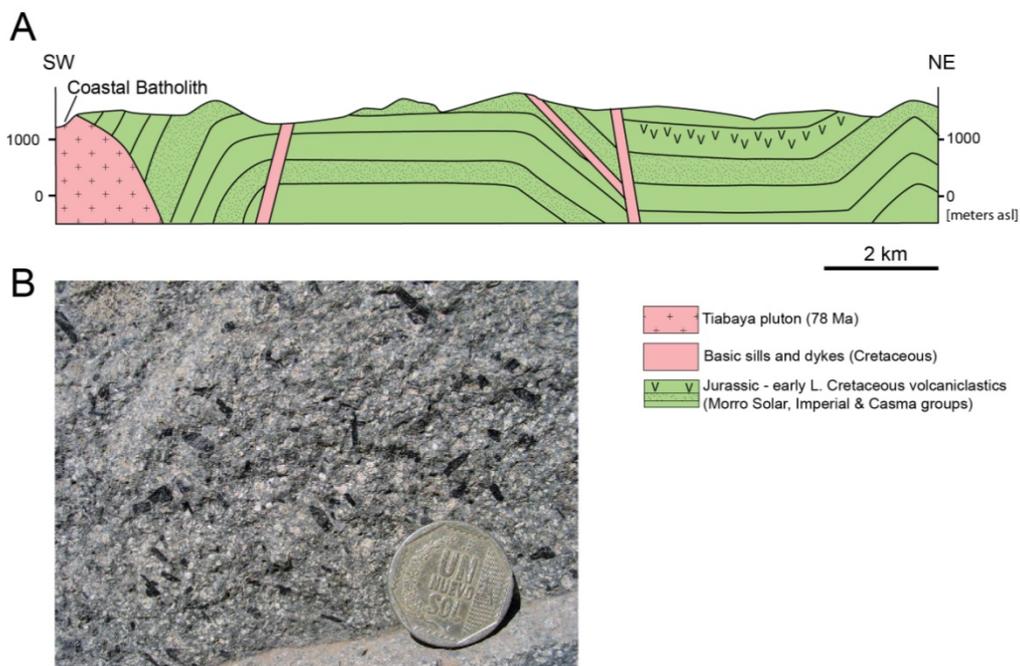

Figure 8. (**A**) Cross-section in the Coastal Belt E–NE of Cañete (see Figure 7 for location). Open folds in the volcaniclastic sequence of the Casma Volcanic Arc are intruded by the Coastal Batholith; (**B**) Photograph of a hornblende diorite from the Coastal Batholith near Lima (11°54.1' S, 76°34.5' W). Hornblende crystals and feldspars are not aligned.

On the eastern margin of the Coastal Belt, Eocene–Miocene volcanic rocks of the Calipuy Group overlie folds and intrusives unconformably. These volcanic rocks can be followed from north to south along the entire Peruvian Andes and from the Pacific coast across the Western Cordillera and locally into the Central Highlands. They conceal the contact between the volcaniclastic sequences of the Coastal Belt and the Mesozoic sediments of the Western Cordillera (see Figure 6). Slight deformation indicated by open folds in the Calipuy Group can be observed in the Western Cordillera and will be discussed in that context.

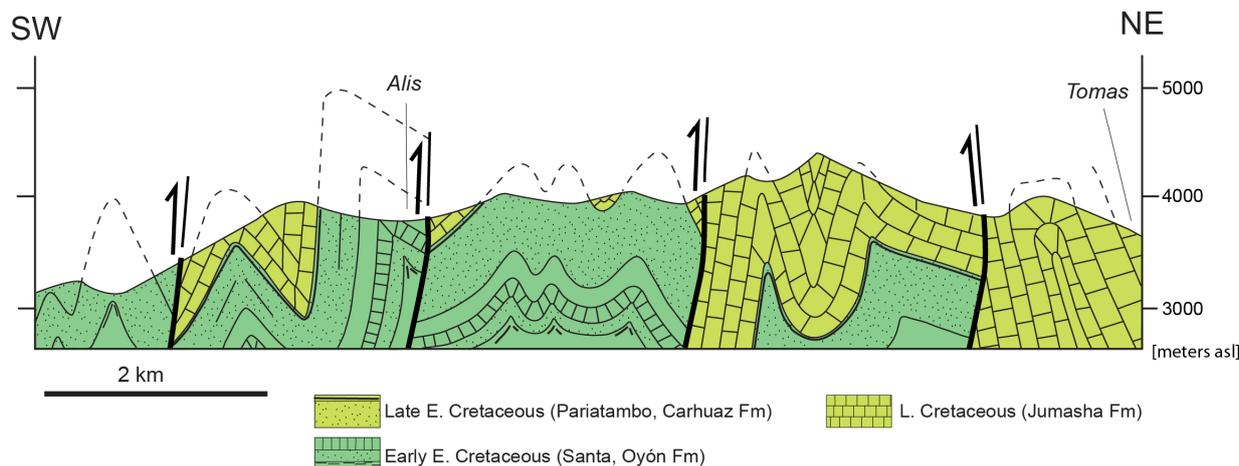### 4.1.2. Western Cordillera

In the Western Cordillera, the most prominent structural province is the Marañon fold-and-thrust belt [17,18]. It forms the core of the Cordillera and consists of highly deformed Cretaceous strata occasionally punctured by small Cenozoic plutons. The main thrust faults are verging to the NE (see Figure 6). The cross-section in Figure 9A displays the internal structure of the Marañon fold-and-thrust belt following the gorge of Rio Cañete between the villages of Alis and Tomas. The Cretaceous strata have been subjected to tight folding resulting in long steep fold limbs and subvertical axial surfaces. The amplitude of the folds exceeds 1 km and some of the folds are isoclinal (e.g., the anticline at Tomas in Figure 9A). Steeply dipping thrust faults put Early Cretaceous shales and sandstones of the Oyón Formation onto the Late Cretaceous limestones of the Jumasha Formation. Given the tight shape of the folds there is no room for Jurassic strata (namely the carbonates of the Chaucha Formation; see Figure 4) in the cores of the anticlines. Rather it must be assumed that the observed folds in the Cretaceous strata are detachment folds. The shales at the base of the Oyón Formation represent the likely detachment horizon at depth.

A different style of deformation within the Marañon fold-and-thrust belt is observed farther north in the Cordillera Raura, 40 km to the west of the city of Cerro de Pasco (see Figure 9B). The Cordillera Raura contains summits reaching up to more than 5000 m and is made up of a stack of thrust sheets of Cretaceous strata. The thrust faults have a relatively shallow dip and are NE-vergent. Within the Cordillera Raura, the tectonic style corresponds to an imbricate stack, whereas to the NE of the cordillera, asymmetric folds dominate the style. Some of them developed thrust faults on their NE limbs. A frontal anticline with a nearly vertical forelimb marks the NE margin of the Cordillera Raura. A thrust fault on this fold limb puts Cretaceous strata onto the undeformed Cenozoic volcanic rocks of the Calipuy Group that in turn unconformably overly the folded Cretaceous strata. This thrust fault raises the top of the Cretaceous strata to higher elevation in the Cordillera Raura. The thrust fault can be traced southward following the eastern margin of the Western Cordillera (Abra La Viuda and San Jose de Quero) as will be discussed below.

Another interesting feature observed in the Western Cordillera are the numerous small intrusions of Cenozoic age that sharply cut the fold structures. In map view they cut across entire fold trains clearly indicating their younger age. At outcrop the intrusive contacts display sharp contacts with the country rocks reminiscent of stoping.

Figure 9. Two cross-sections in the Western Cordillera showing the structural style within the Marañon fold-and-thrust belt. Traces are given in Figure 7. (**A**) Tight folds and steeply inclined thrust faults in the flanks of the Rio Cañete Canyon between Tomas and Alis; (**B**) Imbricate thrusting in the Cordillera Raura.
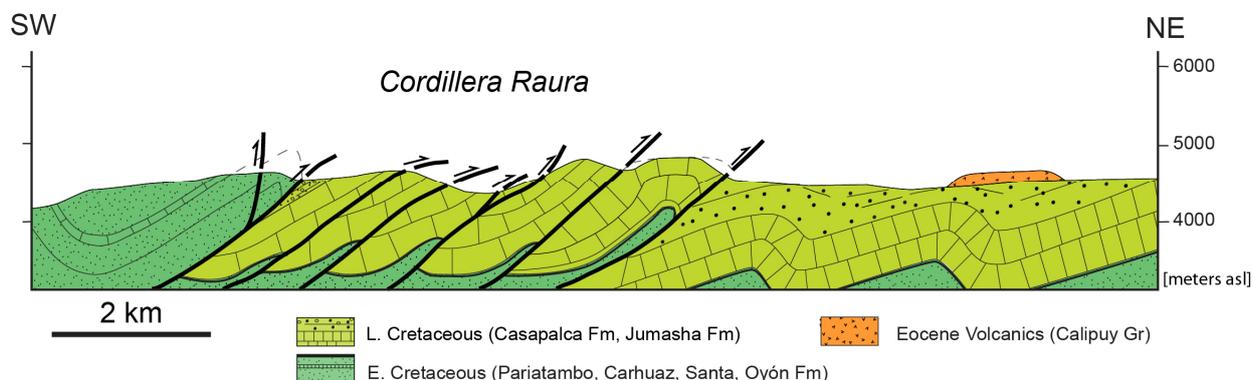

4.1.3. Central Highlands

The area of central Peru between the Western and Eastern Cordillera is characterized by relatively low local relief and elevations not exceeding 4000 m [7]. This high plateau, the Central Highlands, links to the Altiplano of Bolivia in the SE. The structures within the Central Highlands are part of the Marañon fold-and-thrust belt. But unlike the tight folds of the Western Cordillera, folds are more open with larger wavelengths such that they may be recognized on the geological maps at the scale 1:500,000. The cross-section shown in Figure 10 is located between the village of Tomas and Huancayo and highlights the main characteristics. In this part of the Marañon fold-and-thrust belt, the Triassic and Jurassic carbonates of the Pucará Group fill the cores of the anticlines. Owing to the absence of the shales of the Oyón Formation, the entire Mesozoic cover is folded harmonically, a sharp contrast to the neighboring folds in the Western Cordillera (Figure 9A). Generally speaking, the folds become progressively more open going towards the NNE. Near the center of the cross-section shown in Figure 10, limestones of the Jurassic Chaucha Formation form a frontal fold and are thrust onto

tilted and folded Cretaceous strata of the Casapalca and Celendin formations. The displacement along this thrust fault, which we refer to as (San Jose de) Quero fault, amounts to several kilometers. Similar to the situation in the Cordillera Raura (Figure 9B), Eocene volcanics rest unconformably on the folded and eroded Cretaceous strata and are in turn cut by the (San Jose de) Quero fault.

A Neogene intrusion cuts across a broad syncline in Figure 10. Similar crosscutting relationships occur at larger scale and are easily identified on the 1:50,000 geological maps of INGEMMET.

Figure 10. Cross-section of the Central Highlands and the adjacent Western Cordillera between Huancayo and Tomas (see Figure 7 for location). Folds are more open in the Central Highlands. RVQ: Raura–La Viuda–San Jose de Quero fault.
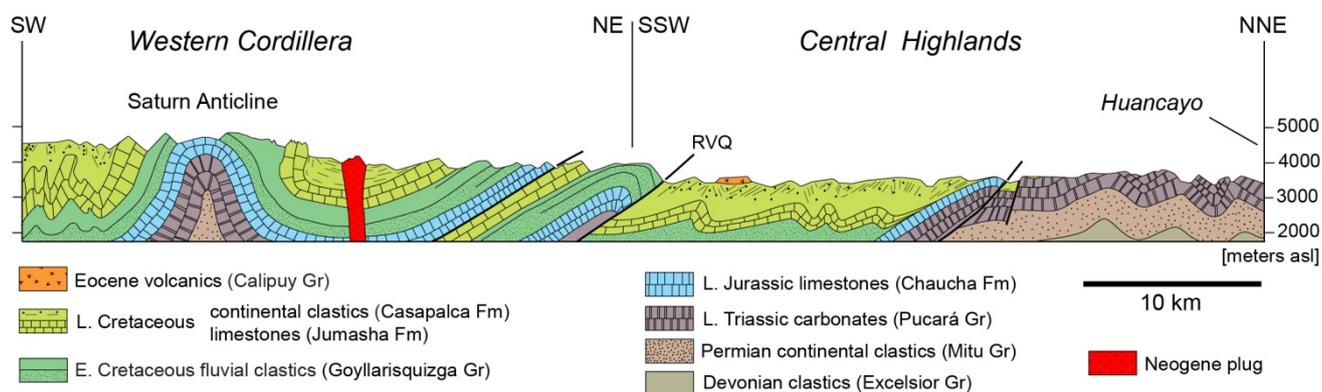

4.1.4. Eastern Cordillera

The core of the Eastern Cordillera is made of Neo-Proterozoic crystalline basement rocks. In the central part, metamorphosed Devonian slates and sandstones (Excelsior Group) overly the basement. The next following Devonian, Late Paleozoic, Triassic and Jurassic strata are shortened by thrusting and folding.

The folds in the Paleozoic and Triassic strata are open with variably oriented axial surfaces and locally subvertical limbs. Steeply dipping faults accompany the folds and give rise to a block-like structural style. On these faults and in the neighboring rocks we observed steeply dipping stretching lineations.

The cross-section in Figure 11A displays the transition from the Central Highlands (Huancayo) to the Eastern Cordillera (Nevado Huaytapallana). A thick sequence of Devonian sandstones and shales, which are internally folded, is thrust westward onto the folded Mesozoic of the Central Highlands. To the E–NE, the Devonian forms an E-vergent anticline with an inverted limb that includes Permian clastics (Mitu Group) and Mesozoic limestones (Pucará Group). The strata on the inverted limb show a cleavage dipping more or less parallel to bedding. A slight metamorphic overprint is indicated by epidote and chlorite in the Devonian and Permian strata and by recrystallization in the Mesozoic limestones. The contact between the Devonian and Permian strata cannot be directly observed in this transect. However, 25 km farther to the northwest, the equivalent contact is marked by an angular unconformity. Towards the east, the inverted limb is in thrust contact to non-metamorphosed Permian red sandstones and conglomerates (Mitu Group) that form an anticline. The recrystallized limestones at the contact display ductile internal folding and a stretching lineation indicating a thrust nature for this contact.

Figure 11. Structural style in the western part of the Eastern Cordillera near Abra Huaytapallana (see Figure 7 for location). (**A**) Cross-section showing folding within the Paleozoic sediments and the Huaytapallana fault juxtaposing Neoproterozoic crystalline basement to the Paleozoic sediments. The Abra Huaytapallana fault is a steep reverse fault with a left-lateral strike slip component; (**B**) Stereoplot of foliation planes (great circles) and stretching lineations indicating strike-slip with thrust component. The northeastern block moved up, placing crystalline basement next to Paleozoic sediments [as shown in (**A**)].
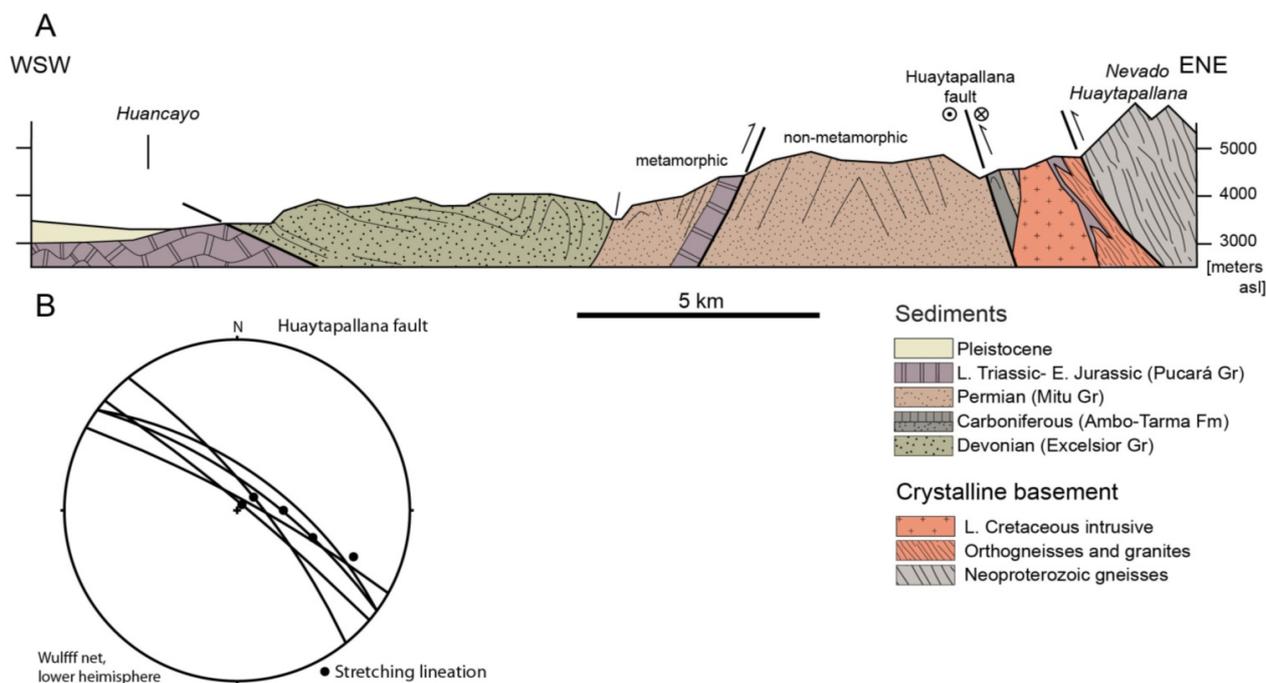
Farther to the E–NE, the anticline formed by the Mitu Group is in contact with a thin band of Carboniferous graywackes, which are in turn overlain by Permian pelites, both units showing a well-developed cleavage. The following zone is a tectonic mélange. The bottom part contains marbles representing highly recrystallized limestones of the Pucará Group. They are intruded by biotite-bearing granites, which correlate with a family of granitic plugs outcropping in this part of the Eastern Cordillera. The granites are Late Cretaceous in age according to the maps of INGEMMET and show no sign of internal deformation while the marbles display flow structures including centimeter-scale sheath folds (see Figure 11B). The sheath folds plunge gently to the ESE. We interpret that the observed recrystallization and folding of these marbles was controlled by heating by the intrusion of the granites.

The upper part of the mélange consists of orthogneisses and granites interlayered with marbles and quartzites. A well-developed cleavage dips parallel to the contacts and carries a stretching lineation with a moderate to steep plunge towards the east and northeast. A sharp NE-dipping tectonic contact marks the limit between the mélange and the Neoproterozoic gneisses to the northeast (see Figure 11A). These gneisses display a prominent subvertical foliation that can be traced into the basement block of the Nevado Huaytapallana.

We interpret that the mélange represents a major fault zone, the Huaytapallana fault, which was responsible for juxtaposing the Neoproterozoic crystalline basement to the Mesozoic and Late

Paleozoic strata. Seismic studies in this area suggest that the Huaytapallana fault is a still active as steeply dipping reverse fault with a strike slip component [4,82]. Our field observations of subvertical and gently ESE dipping stretching lineations corroborate this interpretation and suggest that the Huaytapallana fault is a sinistral (left lateral) transpressional fault.

The Huaytapallana fault can be traced farther to the north. In the vicinity of Comas, a mélange consisting of microgranites, biotite-phyllites and chlorite schists, all overprinted by a homogeneously dipping foliation, separates the Neoproterozoic crystalline basement from Permian strata intruded by Late Cretaceous intrusives. The mélange is up to several 100 m thick and dips steeply to the ENE.

The cross-section in Figure 12 is a transect through the Eastern Cordillera along Rio Perené from Tarma to La Merced. Here, the Neoproterozoic crystalline basement is affected by thrust faulting and folding. At the SW end of the section this basement forms the core of the Tarma anticline. The uplift of the basement in this anticline was aided by two normal faults on either limb of the anticline. Farther to the northeast, three thrust faults successively raise the crystalline basement relative to the neighboring block to the northeast. In each case the sedimentary cover of the basement is preserved in the southwestern portion of the basement block. The steep dip of the thrust faults is reminiscent of a thick-skinned tectonic style if compared to other orogens [85]. The autochthonous cover of Paleozoic and Mesozoic strata, however, is repeated by thrust faulting at several places. This suggests that the Eastern Cordillera is not only block-faulted but rather underwent a considerable amount of shortening. The thickness variations of the individual units indicate synsedimentary faulting in Paleozoic times. For example, the Devonian is restricted to the Tarma anticline and the Mitu Group has a much greater thickness in the central part of the cross-section. These changes are likely to be caused by synsedimentary normal faulting, and these normal faults may well have influenced the ensuing Andean compressional structures.

Figure 12. Structural style in the eastern part of the Eastern Cordillera as observed in the valley flanks of Rio Perené between Tarma and la Merced (see Figure 7 for location).
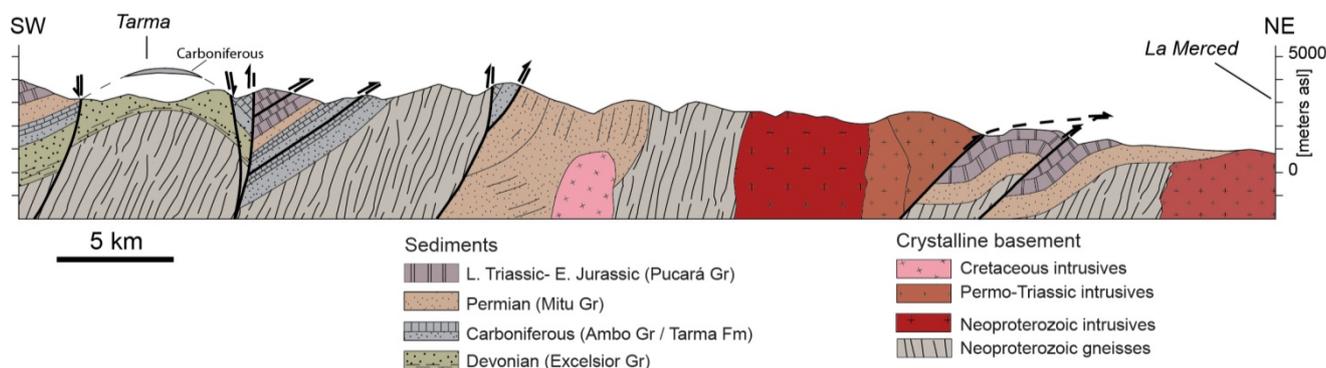
4.1.5. Subandean Zone

Towards the east, the Eastern Cordillera is thrust onto the Subandean Zone along a major thrust fault that put Mesozoic strata and intrusives onto Cenozoic strata of the Amazonas Foreland (see Figure 13). The Subandean zone itself consists of an imbricate stack of thrust sheets involving Paleozoic to Cenozoic strata. In the transect of Figure 13, an antiformal stack can be recognized in the Otishi Cordillera. This structure is particularly well known from seismic and well data acquired for

petroleum exploration [22]. According to these data, Ordovician and Silurian strata form a structural high. East of this structure, in the Amazonas Foreland, thrusting occurred in a westerly direction, suggesting the presence of a triangle zone at the orogenic front.

The detachment horizon for thrust faults in the Subandean zone must most likely be sought in the thick black shale sequence of Carboniferous age (not shown in Figure 13). In contrast, the detachment horizon for the thrust faults of the Otishi Cordillera is located deeper down, most probably in the shales of Ordovician to Silurian age. The continuation of theses thrust faults towards the west and down into the crystalline basement is discussed below in the context of the balanced cross-sections.

Figure 13. Structural style of the Subandean Zone in the area of the Otishi Cordillera (see Figure 7 for location). E–NE-vergent imbricate thrusting prevails in the eastern part adjacent to the Eastern Cordillera. The transition to the Amazonas Foreland is characterized by two WSW-vergent steep thrust faults. Paleogene–Neogene sediments were deposited in foreland basin.
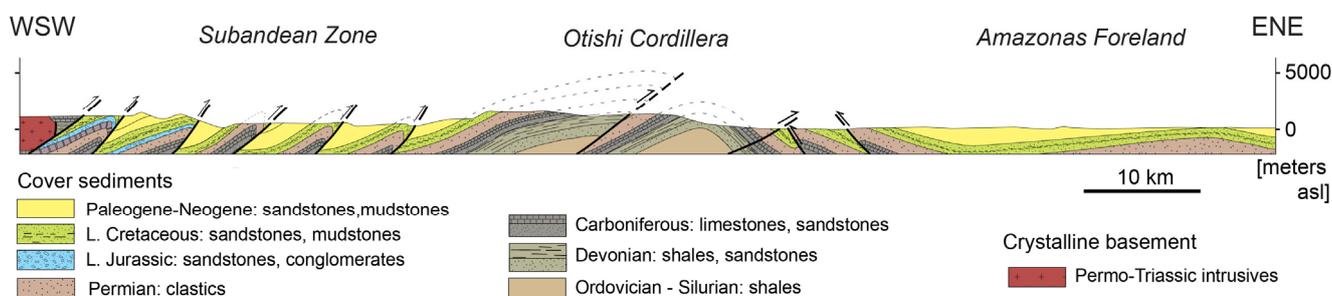
4.2. Balanced Cross-Sections

In order to have a complete structural model of the Central Peruvian Andes, two regional balanced cross-sections were constructed, one in the north passing the town of Huaraz, one in the south passing the town of Huancayo (see Figure 7 for location). Both cross-sections start at the Pacific coast and end in the Amazonas Foreland. The direction was chosen perpendicular to the main trend of the orogen and more or less parallel to the tectonic transport direction. These balanced cross-sections are based on our own field observations, topographic and geological maps at the scale 1:100,000 of the Peruvian geological survey (INGEMMET), as well as published seismic sections of the area [22]. The interpretation at deeper level was done using modern tools of structural geology and a mechanical stratigraphy extrapolated from known stratigraphic sections within the Andes. Both cross-sections are approximately 390 km long.

The balancing of the cross-sections was done to fulfill the generally accepted rules:

(1) The cross-sections need to be viable, meaning that they reflect the general structural style of the orogen. This style is illustrated and discussed in the preceding Section 4.1 (see Figures 8–13).

(2) The cross-sections need to be retro-deformable. To achieve this, line length balancing [86] was performed using mechanically strong layers as reference horizons. Owing to significant thickness changes across the orogen, volume balancing is rendered very difficult if not impossible.

(3)   The interpretation at depth, including the determination of the "depth-to-detachment", was performed using concepts described in [87] for thrust systems and models for detachment folding [88,89].

(4)   Displacements along faults must be consistent, *i.e.*, they cannot change without reason. Displacement variations can be caused by stretching and/or shortening in the hanging wall and footwall rocks, or by merging or branching splay faults [90].

(5)   In 2D-balancing the trace of the cross-sections should not cross faults with movements in and out of the cross-section. We could not avoid such circumstances and treated the segments individually.

4.2.1. Southern Traverse

The balanced cross-section shown in Figure 14 referred to as Southern Traverse in this paper, spans from the town of San Vicente de Cañete on the Pacific coast to Huancayo in the Central Highlands and on to Rio Urubamba in the Amazonas jungle (see Figure 7 for location). The section was divided into four segments for balancing: the Coastal Belt with the deformed Casma Volcanic Arc sequence, the western part of the Western Cordillera with its highly deformed Mesozoic sequence, the Central Highlands and adjoining parts of the Western and Eastern Cordilleras where Paleozoic and Mesozoic strata are affected by shortening, and, the Subandean Zone including parts of the adjoining Eastern Cordillera.

Within the Coastal Belt the cross section displays long wavelength open folds of the Early Cretaceous volcaniclastic Casma group and equivalents. Shortening within these folds amounts to 20–30 km. The preferred value of 25 km corresponds to 28% shortening. The folds are intruded by the tabular bodies of the Coastal batholith, which we show bounded by vertical faults. These faults allowed the uprising of the magmas to higher levels of the crust and subsidence of the floor of the intrusion, a mechanism discussed above in Section 3. The intrusions in the west are of Late Cretaceous, the ones in the east of Oligocene age. The basement of the Casma Group and equivalents is exposed along the Pacific coast in the so-called Arequipa massif, an assemblage of high-grade partly migmatized gneisses and schists that are intruded by Early Paleozoic granites [15]. In our cross-section we show the volcanic arc and the underlying continental crust of the Arequipa massif to be thrust onto the South American craton and parts of its deformed sedimentary cover and assume that this thrusting occurred in the course of the amalgamation of the volcanic arc to the craton. The rocks of the Arequipa massif were seemingly hardly deformed in this process [15].

Figure 14. Southern Traverse: This balanced cross-section runs from the Pacific coast (Cañete) to Huancayo, the Otishi Cordillera and into the Amazonas Foreland. The trace is shown in Figure 7. RVQ: Raura–La Viuda–San Jose de Quero fault. See text for discussion. An enlarged version of this figure is available in the supplementary material (Figure S2).
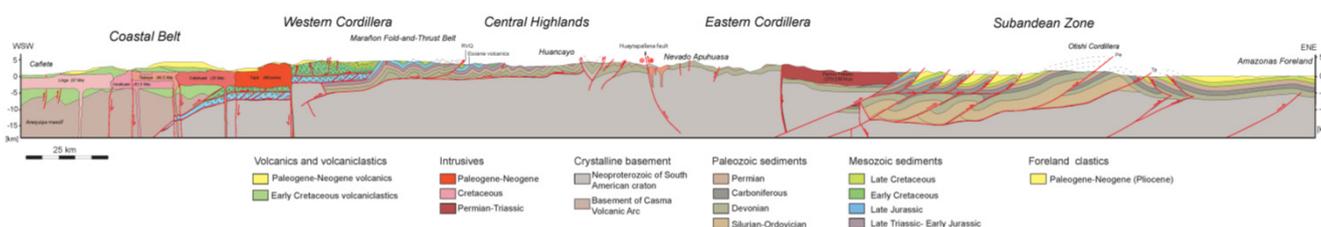
A completely different style is encountered in the Marañon fold-and-thrust belt of the Western Cordillera. In its western part, Cretaceous strata are isoclinally folded. The tight folds require a detachment horizon that most likely is located in the shales and coal bearing strata of the Oyón Formation as already suggested by [17]. We suspect that Jurassic strata are present at depth similar to the situation in the eastern part of the Western Cordillera. In our construction we postulate a detachment horizon following the shales of the Oyón Formation. We interpret this detachment fault as roof thrust of a duplex structure within the underlying Jurassic sediments and added the typical imbricate thrusts and folds expected in the carbonates of the Chaucha Formation. Even if this structure is hypothetical, the Jurassic strata restore to the same bed-length and accommodated the same amount of shortening as the Cretaceous strata. The western termination of the isoclinally folded Cretaceous strata at depth is projected from map data. It corresponds to the westernmost outcrops of Cretaceous strata found along strike farther to the NNW. The western termination of the underlying Jurassic strata then followed from bed length balancing and presents a plausible solution. Our construction yields a total shortening of 45–60 km for this western part of the Western Cordillera, 35 km of which corresponds to the strata outcropping within the cordillera itself. The preferred value of 55 km corresponds to 62% shortening.

The folds in the eastern part of the Western Cordillera are more open and have larger wavelengths. Farther to the NNW, near La Oroya, Paleozoic and Triassic sediments are found in the core of the open folds in the Western Cordillera and testify to a harmonic folding of not only Jurassic and Cretaceous, but also Paleozoic strata. Regarding the absence of a detachment between the Jurassic and Cretaceous strata, the change in style may be attributed to a rapid primary thickness decrease of the Oyón Formation going east.

The style of relatively open folds involving Paleozoic and Mesozoic strata continues into the adjoining Central Highlands and even into the Eastern Cordillera. The boundary between Western Cordillera and Central Highlands is marked by a major thrust fault, the San Jose de Quero thrust, whereas the boundary between Central Highlands and Eastern Cordillera is more transitional. ENE of Huancayo (see Figure 14), the Neoproterozoic basement is uplifted to the surface by thrust faults and a major fault, the Huaytapallana fault, juxtaposes a large basement block to Late Paleozoic sediments, implying a vertical offset of several kilometers. As discussed above (Figure 11), the Huaytapallana fault has a sinistral strike-slip component, which has to be considered in a 3D retro-deformation, but which is difficult to reconcile in 2D line-length balancing.

The thrust faults affecting the Paleozoic and the Mesozoic strata in the Western Cordillera and the Central Highlands exposed at the surface are located in the Devonian phyllites. We interpret that they emerge from a sole fault in the subsurface is also following the Devonian phyllites as detachment horizon. The folds in the Paleozoic sequence of the Eastern Cordillera are more open and affect also the Neoproterozoic basement. The structure beneath the Permo–Triassic intrusion is nowhere exposed and therefore speculative. Nevertheless, the cutoff at the major thrust fault beneath the Permo–Triassic intrusion was taken as eastern pin line for balancing. Since the Paleozoic strata extend all the way across this segment, we used the Devonian as reference horizon for balancing and obtained a total shortening of 20–35 km, with a preferred value of 26 km (13.5%).

The Subandean Zone and the adjoining Eastern Cordillera show a very different tectonic style. The main characteristics comprise imbricate E-vergent thrusting. Within the Eastern Cordillera, an

important thrust fault uplifted the Permo–Triassic batholith that intruded Early Paleozoic sediments and juxtaposed it to the Late Cretaceous deposits of the Subandean Zone. The base of this intrusion is nowhere exposed, such that the Devonian sediments shown in Figure 14 are speculative.

Between the Permo–Triassic intrusion and the Otishi Cordillera, the style is dominated by imbricate thrusting that affects the Neogene deposits of the Amazonas Foreland. Reflection-seismic sections and borehole data [22] reveal that a detachment horizon is located in the shale of the Early Carboniferous Ambo Formation. Deeper down, a duplex of Ordovician to Devonian strata has a floor thrust in Ordovician shale. The roof thrust is shared with the overlying imbricate stack. In the Otishi Cordillera, the floor thrust climbs section. One branch, the Perené–Cuitivireni thrust of [22], puts Devonian onto Permian strata, the second branch, the Tambo fault of [17], carries a large anticline in its hanging wall. This anticline may well represent a fault-bend fold, which formed as a consequence of the ramp that the thrust followed. E–NE of the Otishi Cordillera, two W-vergent thrust faults can be recognized, and finally, in the Amazonas Foreland, a broad anticline is observed at the surface and may well be associated with a thrust fault in its core. It is important to note that in the Amazonas Foreland, Late Cretaceous strata rest directly on Permian deposits and the Devonian sediments overly crystalline basement. It seems thus likely that the ramp beneath the Otishi Cordillera was controlled by Early Paleozoic synsedimentary normal faults. The Early Paleozoic is also absent west of the Permo–Triassic intrusion in the Eastern Cordillera, such that an additional basin-bounding fault must be suspected at depth. Our construction assumed this fault to be at the eastern margin of the intrusion. The total shortening we obtained for this segment amounts to 40–50 km with a preferred value of 42.3 km (24%).

Summing up, we estimate that the Southern Traverse was shortened by roughly 150 km (28%) from an original length of 545 km. Minimum and maximum estimates of shortening are 125 and 174 km.

4.2.2. Northern Traverse

The Northern Traverse shown in Figure 15 runs from approximately Huarmey at the Pacific coast across the Cordillera Negra and Blanca into the Amazonas Foreland north of Tingo Maria (see Figure 7 for the exact location of the trace). For convenience, the profile is subdivided into four segments (Coastal Belt, Western Cordillera, Eastern Cordillera and Subandean Zone), which will be addressed individually.

Figure 15. Northern Traverse: This balanced cross-section runs from the Pacific coast (Casma) to Huaraz into the Amazonas Foreland. The trace is shown in Figure 7. See text for discussion. An enlarged version of this figure is available in the supplementary material (Figure S3).
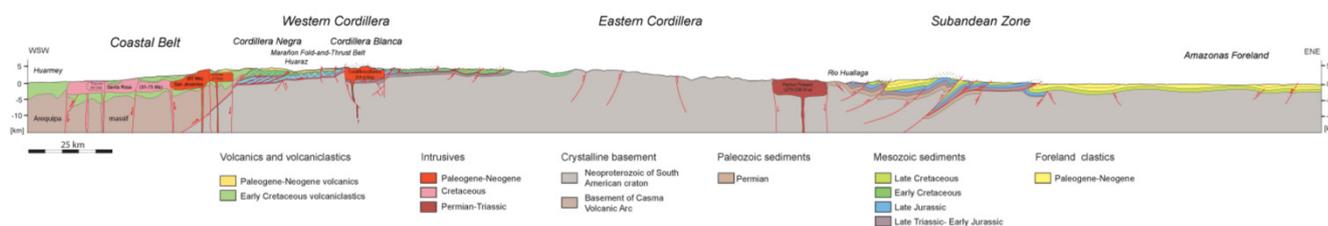
The volcaniclastics of the Casma Group in the Coastal Belt display gently asymmetric open folds with rounded hinges. Locally vertical faults crosscut the folds. We infer the existence of a thrust fault at depth that formed during amalgamation of the Casma Volcanic Arc to the South American craton and its cover, the Marañon fold-and thrust belt. Our retro-deformation suggests a shortening of 15 to 20 km with a preferred value of 17 km (28%) within the Coastal Belt. Cretaceous and Cenozoic magmatism produced the tabular bodies of the Coastal Batholith. Steep faults at the margin of individual plutons allowed floor subsidence during the intrusion process as discussed above in Section 3.

The Western Cordillera encompasses the Cordillera Negra and the Cordillera Blanca, both of which are part of the Marañon fold-and-thrust belt. Within the Cretaceous strata, upright and slightly asymmetric folds characterize the tectonic style. Both rounded hinges and box folds are observed. In the Cordillera Negra, the tight folds in the Cretaceous strata suggest a detachment in the shales of the Oyón Formation, similar to the Southern Traverse (Figure 14). We interpret that Jurassic strata are present beneath the detachment horizon and suggest shortening by imbricate thrusting in the Jurassic carbonates and a basal detachment in the evaporites of the Pucará Group. A thick layer of volcanic rocks of the Calipuy Group overlies the folded Cretaceous strata. However, in some of the deeply incised valleys the style shown in Figure 15 can be observed at outcrop.

Glacial and fluvial Pleistocene and Holocene deposits cover the Mesozoic strata and the volcanic rocks between Rio Santa and the Cordillera Blanca Batholith. We infer that in this segment the Jurassic and Cretaceous strata are folded harmonically, similar to the style observed just east of the Cordillera Blanca Batholith. The detachment for these folds is postulated in the evaporites of the Pucará Group. A major vertical fault marks the western limit of the Cordillera Blanca Batholith. During the emplacement of the batholith, this fault allowed floor subsidence such that the eastern block subsided. But later, the Cordillera Blanca Batholith was uplifted more or less along the same fault relative to the highly deformed Mesozoic strata to the west. The fault and evidence for its motion can be observed at outcrop (see Figure 13 in [7]); displaced Quaternary gravel terraces testify to a very young activity along this fault. The net displacement along the fault as shown in Figure 15 amounts to 3 km.

On the eastern border of the Cordillera Blanca Batholith, the granites intruded the harmonically folded Jurassic and Cretaceous strata. Stoping structures can be seen at several locations and also in the roof of the batholith. Farther East, a roughly 10 km wide segment contains tight folds within the Cretaceous strata that suggest a detachment in the shales of the Oyón Formation. The adjacent segment to the East is dominated by more open folds, which are cut by E-vergent thrust faults. Finally, the crystalline basement is overlain unconformably by an autochthonous cover (Cretaceous along this transect, Late Paleozoic farther north) and is affected by long wavelength folds. The total amount of shortening within the Cretaceous strata in the Western Cordillera is 30 to 40 km with a preferred value of 35.5 km (26%) according to our construction.

In the Eastern Cordillera, the crystalline basement is exposed at an altitude of about 4000 m above sea level. Its sedimentary cover has been removed by erosion. The Permo–Triassic intrusives at the eastern side of the Eastern Cordillera shows no signs of internal deformation. Thus one could be attempted to interpret that the Eastern Cordillera has been uplifted by the thrust faults just east of the intrusion as a "block". Instead, we use the cross section from Tarma to La Merced shown in Figure 12, which involves Paleozoic sediments, to get an estimate of the shortening within the Eastern Cordillera. Outcrop conditions on the flanks of the deeply incised Rio Perené constrain the construction of a

cross-section, from the retro-deformation of which we obtain a shortening of 40 to 55 km with a preferred value of 46 km (39%).

Farther east, several west-dipping thrust faults affect the Paleozoic, Mesozoic and Cenozoic strata. The thrust faults raise the top-crystalline basement contact to successively higher levels. In the central part of the Subandean Zone, a detachment within the evaporites of the Pucará Formation must be assumed. It puts the Triassic to Jurassic strata onto the Neogene sediments. Farther east, within the Amazonas Foreland, gentle folding affects the Neogene and Pliocene sedimentary cover. Reflection-seismic data suggest that the crystalline basement is also slightly warped. The Cretaceous strata of the Subandean Zone suggest a shortening of 22 to 30 km with a preferred value of 24.7 km (14%).

For the entire balanced cross-section, an estimate for total shortening of 120 km from an original length of 508 km is obtained, less than the 150 km determined for the Southern Traverse. Minimum and maximum estimates of this total shortening amount to 107 and 145 km.

The two balanced cross-sections are of nearly equal length in the present day deformed state (388 km for the Northern Traverse, 396.4 km for the Southern Traverse). The retro-deformed state of the two balanced cross-sections shown in Figure 16 reveals that the Southern Traverse is longer than the Northern Traverse (545 *vs.* 508 km). This is in concert with the difference in total shortening that amounts to 150 km (28%) for the Southern and only 120 km (24%) for the Northern Traverse. Closer inspection shows that the Subandean Zone underwent less shortening (14% in the Northern and 24% in the Southern Traverse) as compared to the roughly 30% obtained for the Western and Eastern Cordilleras combined and the 28% for the Coastal Belt.

The retro-deformed sections in Figure 16 also highlight the architecture of the Paleozoic, the Mesozoic and the Cenozoic basins. In the Northern Traverse, a Late Paleozoic basin is present in the Eastern Cordillera, while the Mesozoic W-Peruvian basin is restricted to the Western Cordillera. This basin geometry explains the difference in structural style between the two cordilleras. The steep reverse faults in the Eastern Cordillera, which are in part transpressive structures, contrast to the fold-and-thrust structure underlined by a major detachment in the Western Cordillera.

In the Southern Traverse, an Early Paleozoic basin is recognized in the Subandean Zone and may have contributed to the imbricate thrust structures. The western termination of this basin corresponds structurally to the abrupt transition between the Subandean Zone and the Eastern Cordillera where the top of the crystalline basement has been uplifted along a major thrust fault. We suspect that this thrust fault was somewhat controlled by the basin bounding fault. A Late Paleozoic basin stretched across the Eastern Cordillera and the Central Highlands into the Western Cordillera. Upon inversion of this basin, relatively open folds and steep reverse faults developed. Some of the steep faults are of transpressive nature. The Mesozoic strata of the W-Peruvian basin were intricately folded upon inversion. The presence of a detachment horizon in the Oyón Formation allowed the folds to become almost isoclinal and to deform independently from the underlying Late Triassic and Jurassic strata.

The Cenozoic basin of the Amazonas Foreland was in part incorporated into the orogen (Subandean Zone). Its western termination corresponds to the eastern border of the "Marañon geanticline", a structural high that spans the Eastern Cordillera and separated the W-Peruvian from the E-Peruvian basin [18,91]. Here too, pre-existing structures had a significant influence on the development of the Andean structures.

Figure 16. Retro-deformed cross-sections of the Northern and Southern traverses. Retro-deformed lengths, shortening and actual lengths are given in kilometers. The restored sections show the geometry of the Paleozoic, Mesozoic and Cenozoic basins. An enlarged version of this figure is available in the supplementary material (Figure S4).
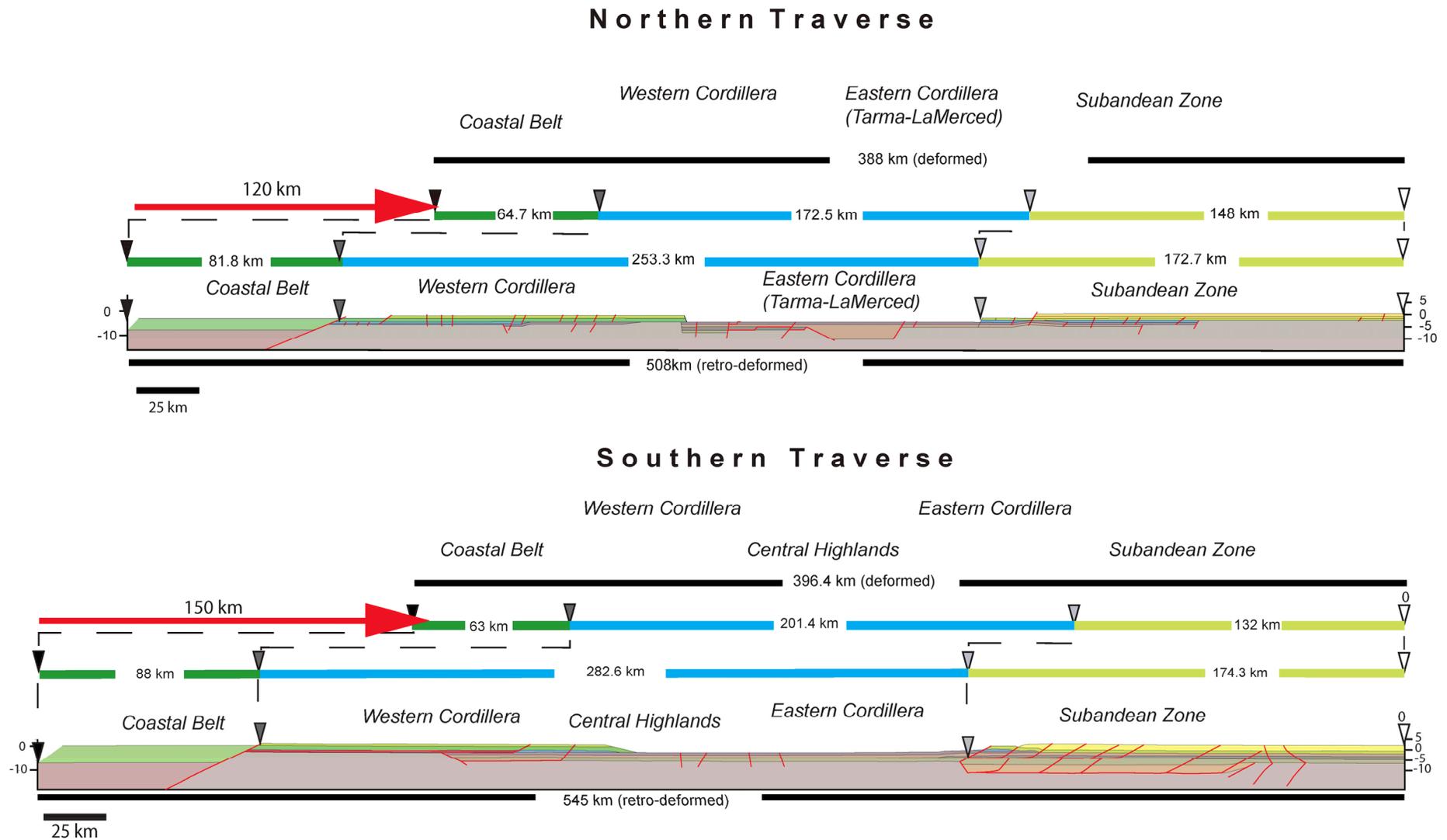
5. Structural Evolution

The structural analysis and the balanced sections in the preceding chapters serve as basis for the discussion of the structural evolution of the Central Peruvian Andes. Important arguments for the timing of events stem from unconformities and the intrusive contacts of the plutons as observed in the field.

Previous workers have already recognized a succession of orogenic deformation phases in the evolution of the Peruvian Andes. These include [17–20,74,91–93] just to mention a few. All of these studies refer to the pioneering work of Steinmann [16] who was the first to establish a succession of structural events and also attributed names to these phases. He defined four phases in the Central Peruvian Andes: the Late Cretaceous Mochica and Peruvian Phases, the Eocene Inca Phase and the Miocene–Pleistocene Quechua Phase. Some authors correlated these phases, which originally were thought to represent compressional events, to different magmatic pulses or even tectono-magmatic events (e.g., [62]).

In the following we will restrict the term of "phase" to deformation events that produced folds and/or faults recognizable at outcrop. As a consequence, the "Peruvian phase" is not used in this paper. The "Peruvian phase" is marked by a change from marine to continental conditions in the W-Peruvian trough in Late Cretaceous times caused by basin scale vertical movements in the wake of the accretion of the Piñon terrane in the neighboring Northern Andes [20]. We illustrate the observed structures that pertain to individual deformation phases in detailed cross-sections from various parts of the orogen. At this point it is important to note that deformation phases as defined by deformation structures give the relative timing of events and do not imply chronological ages. In fact in the case of a fold-and-thrust belt that develops by in-sequence thrusting, deformation is diachronous on a regional scale. Nevertheless time brackets based on ages of sediments and magmatic rocks will be discussed where possible to constrain the evolution in time.

5.1. Mochica Phase

The Mochica Phase corresponds to the deformation event that led to the open folds visible in the Casma Group of the Coastal Belt. In many instances these folds have straight limbs and relatively sharp hinges. We could not observe any consistent cleavage related to these folds. Similarly, [15] report that there is no penetrative deformation of Late Paleozoic and Mesozoic age discernible in the underlying crystalline basement of the Arequipa massif. The folds are sharply cut by the Coastal Batholith as well as associated dykes and sills (see Figure 17). The age of the Mochica Phase can be bracketed between the youngest strata folded (Albian for the Casma Group; *ca*. 100 Ma) and the intrusion age of the Coastal Batholith (95 Ma for the Paccho, 91 Ma for the Santa Rosa unit) in the case of the area just N of Lima [60,61]. [30] showed that in the Lima area, magmatism and sedimentation continued up into the Late Cretaceous and were accompanied by dextral strike-slip faulting related to oblique folding.

Figure 17. Deformation features linked to the Mochica Phase in the Coastal Belt in a cross-section from Santa Rosa to Canta (see Figure 7 for location).
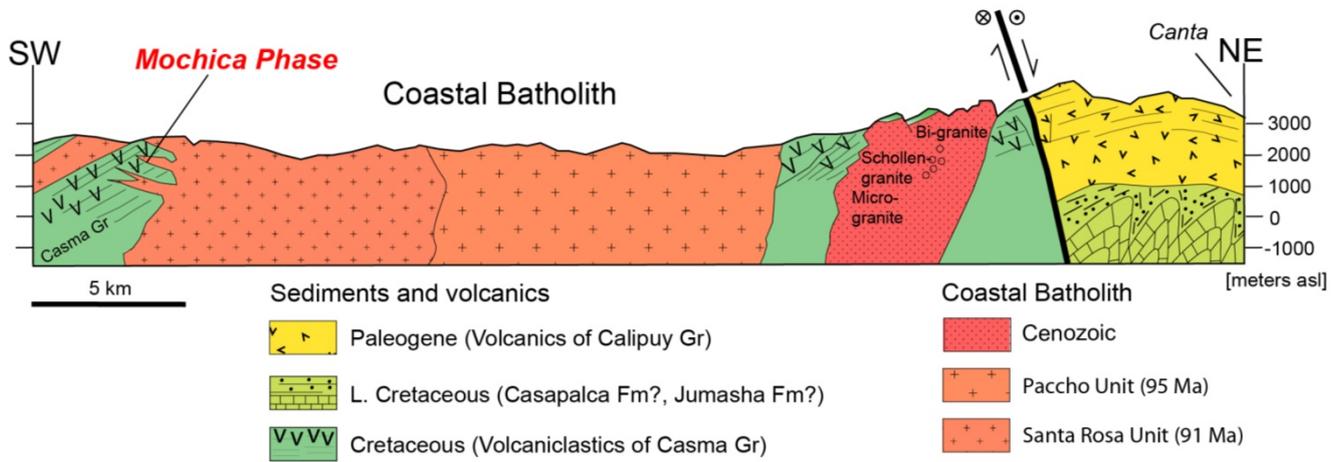
5.2. Inca Phase

The Eocene Inca Phase encompasses the tight folding and thrust faulting of the Mesozoic strata in the Western Cordillera and the more open folding and und steep thrust faulting in the Paleozoic–Mesozoic strata of the Central Highlands and the adjacent Eastern Cordillera. The tight, sometimes nearly isoclinal folds do not show a penetrative cleavage. Field observations reveal local faulting and brecciation in the hinges of folds. Viewed at large scale, the Marañon fold-and-thrust belt can be attributed to the Inca Phase deformation. The youngest sediments affected by these folds and thrusts pertain to the Late Cretaceous continental deposits of the Casapalca Group (90–65 Ma). A spectacular unconformity gives the upper time bracket for the Inca Phase. Eocene–Oligocene (33 Ma) volcanic rocks [59,73,74] of the Calipuy Group overlie the eroded Marañon fold-and-thrust belt along the entire Western Cordillera. Figure 18A shows the unconformity in a cross-section through the Cordillera Negra in the north of our study area. Here, the Cretaceous strata are partly isoclinally folded and the unconformity points to substantial erosion and paleo-relief prior to the deposition of the volcanics. This paleo-relief may well be responsible for local variations in dip of the volcanic flows. A photographic view of the unconformity as seen in the area of the Southern Traverse (near the village of Laraos, SE of Rio Cañete) is given in Figure 18B.

Figure 18. Deformation features linked to the Inca Phase in the Western Cordillera. (**A**) Cross-section in the Cordillera Negra west of Huaraz (see Figure 7 for location). Pre-Cretaceous strata in the Cordillera Negra are nowhere exposed and thus speculative; (**B**) Photograph of the "Great unconformity" at the base of the Calipuy Group in the Cerro Patille (12°27' W, 75°40' W) SE of Laraos. Looking SE; width of photograph *ca.* 2 km.
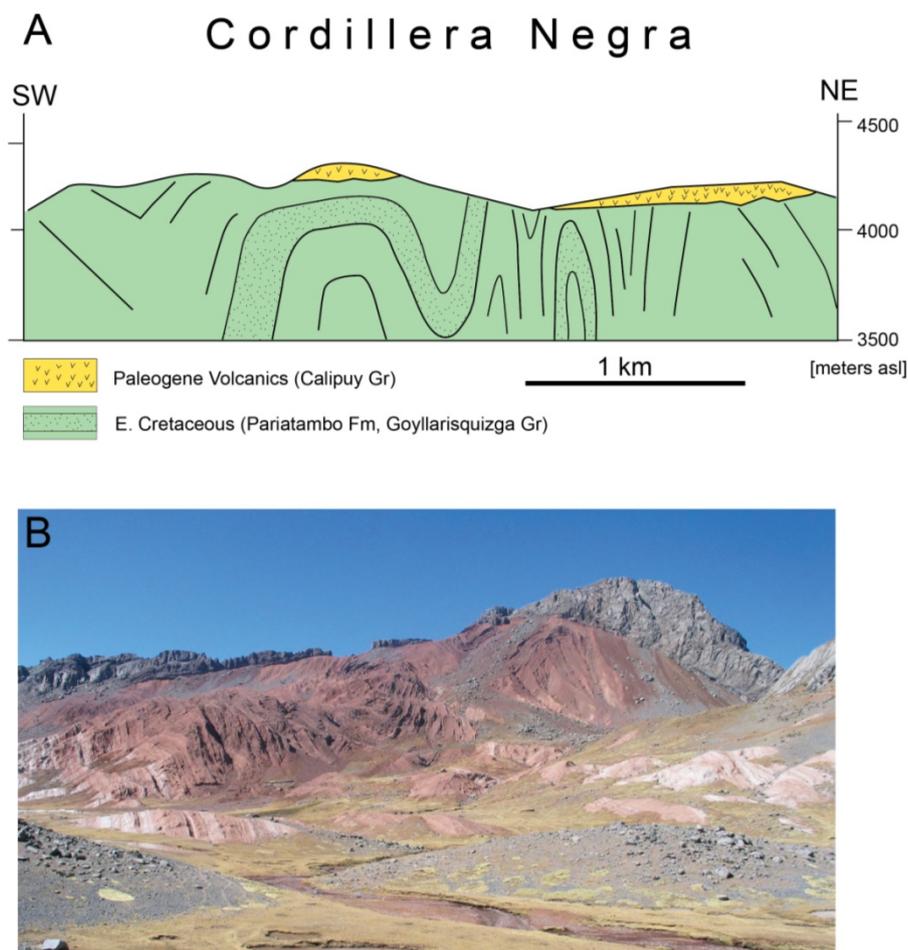

5.3. Quechua Phase(s)

Although the Quechua Phase is mostly discussed in the framework of the Subandean Zone and Eastern Cordillera, we found evidence for post-Eocene thrusting in the Western Cordillera, too. In the following discussion we will proceed from west to east, from the Western Cordillera to the Subandean Zone. Based on stratigraphic dating, several episodes were differentiated within the Quechua Phase and numbered from 1 to 3 by [18] and in the review by [20]. These authors correlate the Quechua 1 episode with uplift in the Eastern Cordillera of Ecuador, reactivation of Inca Phase structures in the Western Cordillera of Peru and monoclinal folds and reverse thrusts in southern Peru in the time span 17–15 Ma. The Quechua 2 episode (9–8 Ma) on the other hand was held responsible for thrusting of the "Paleo-Andes" to the NE resulting in a restriction of sedimentation to the margins of the orogen. The Quechua 3 episode, finally, occurred in the time interval between 7 and 5 Ma and was correlated to the formation of the Subandean thrust belt. Besides the sediments in the Subandean Zone, the volcanic sequences of the Calipuy Group and equivalents represent important markers for the timing of

the structural development. These rocks were deposited between the late Eocene and the Miocene. They overly the deformed Cretaceous sediments as discussed above. In most instances, the volcanic sequence has a sub-horizontal layering implying little or no deformation after their deposition. However, an angular unconformity can locally be observed at the base of the Miocene lava flows. Tilting of the older volcanic deposits is attributed to an episode of the Quechua Phase. Additional information on these features can be found in [73,75,76].

Figure 19. Deformation features linked to the Quechua Phase in the Western Cordillera and the Central Highlands (see Figure 7 for location). (**A**) Cross-section Canta–Abra La Viuda showing Quechua Phase thrusts uplifting the Western Cordillera. RVQ: Raura–La Viuda–San Jose de Quero thrust; (**B**) Cross-section of the Cordillera Blanca east of Huaraz showing uplift of the Cordillera Blanca Batholith relative to the folded Mesozoic units to the SW. CBDF: Cordillera Blanca detachment fault; (**C**) Cross-section of folded Pleistocene gravels in the Central Highlands west of Huancayo.
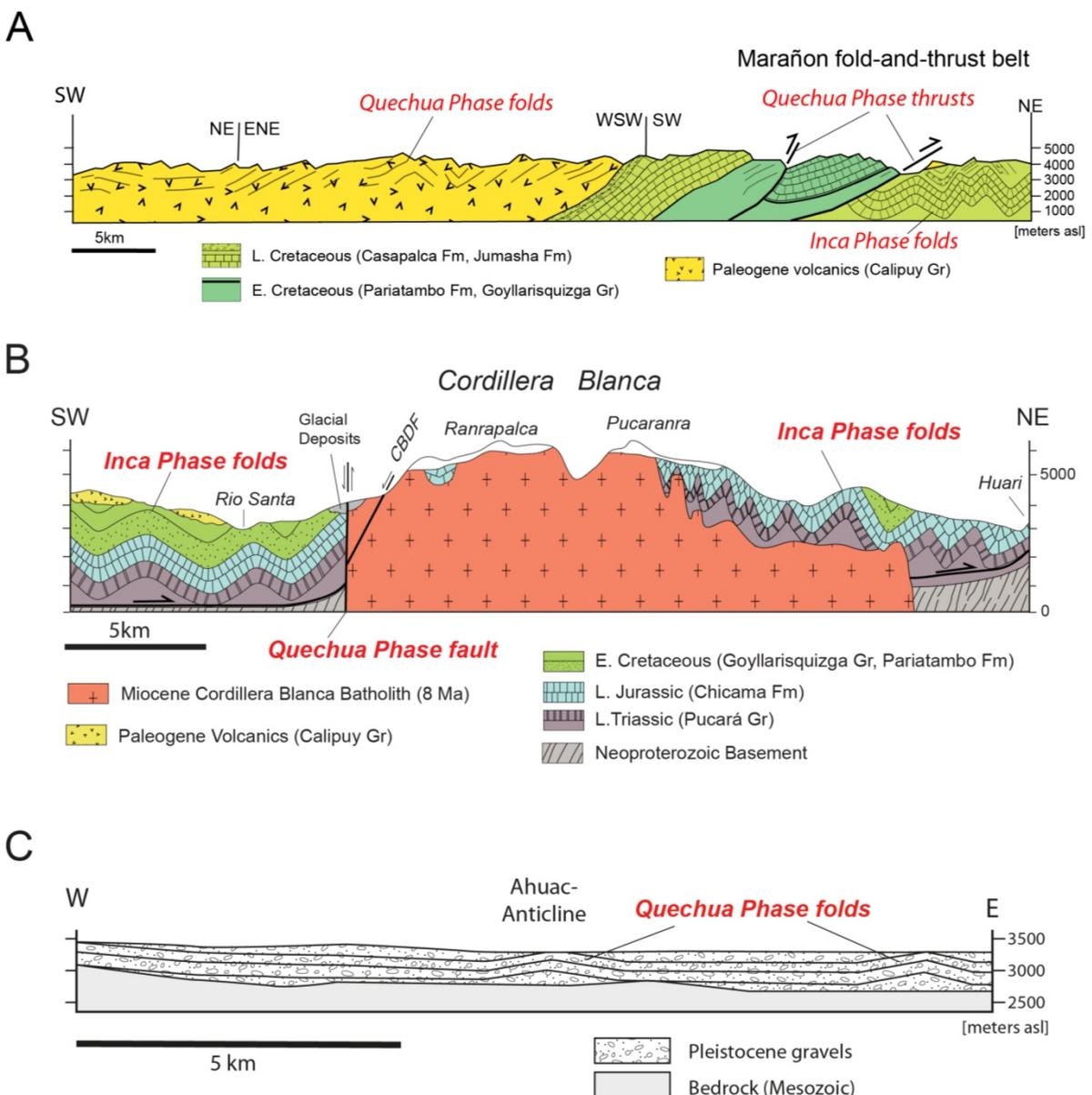
In the transect Canta to Abra la Viuda located north of Lima, the Eocene–Oligocene volcanics of the Calipuy Group are gently folded (Figure 19A). NE of Abra la Viuda, on the Central Highlands, the volcanic deposits overly the folded Cretaceous of the Marañon fold-and-thrust belt unconformably as discussed earlier. However, a major thrust fault breaking surface at Abra la Viuda cuts the unconformity and raises the Cretaceous strata of the Western Cordillera above the volcanics of the Central Highlands.

This thrust fault (and associated splays) can be followed from Abra la Viuda to the NW to the Cordillera Raura (W of Cerro de Pasco) as well as to the SE to San Jose de Quero (W of Huancayo) as a series of thrust faults aligned in an en echelon pattern. We refer to this thrust-fault system as the Raura–La Viuda–(San Jose de) Quero (RVQ) fault system. The situation in the Cordillera Raura has already been discussed in the framework of structural styles in Figure 9, and the situation near San Jose de Quero in Figure 10 (see Figure 7 for locations).

An additional reverse fault with considerable offset follows the SW margin of the Cordillera Blanca. It raised the Cordillera Blanca batholith that intruded in Miocene and Pliocene times by several kilometers relative to the adjacent Cordillera Negra (Figure 19B). Part of this uplift occurred in the context of the intrusion of the Cordillera Blanca Batholith. As discussed in [7], the Cordillera Blanca detachment fault (CBDF in Figure 19B), which manifests itself by a WSW dipping 1 km thick mylonite belt [94], is suspected to be a syn-intrusion normal fault that accommodated the rise of the central part of the batholith, comparable to structures such as known e.g. in the Alps ("Pedra Rossa shear zone" of [95] in the roof of the Bergell pluton). This interpretation is in contrast with previous workers who interpreted this fault as a low-angle detachment representing a regional extensional event [95,96] related to buoyancy and gravitational collapse of high mountains. Our observations show that the fault, which marks the contact between the batholith and the encasing rocks, is nearly vertical (Figure 13 in [7]). Slickensides on the fault surface are down-dip and suggest uplift of the northeastern block (the batholith). Moreover, several faults nearby, which cut and displace Pleistocene moraines and Holocene fluvial cones, are also sub-vertical and uplift the northeastern block. A detailed description of these faults is given in [97]. On aerial photographs shown in his Figure 3, the traces of the faults rupturing the surface are straight across valleys and ridges and clearly indicate that the faults are sub-vertical. In any case, the surface ruptures indicate a very young age for the last episode of Quechua Phase activity of these faults.

Quechua Phase deformation in the Subandean Zone encompasses imbricate thrusting that affected sediments as young as Pliocene in age. In the cross-sections shown in Figures 13 and 14, the youngest sediments in the internal thrust sheets are of Miocene age (Chambira Formation), whereas in the external thrust sheets, Pliocene sediments (Ipururo Formation) are involved. This suggests that within the Subandean Zone, Quechua Phase thrusting was in-sequence thrusting that migrated in time towards the foreland in a northeasterly direction. GPS-data [98,99] suggest that these movements are still ongoing.

In the area of Huancayo, Pleistocene gravels were deposited in the Central Highlands. Pebble spectra show that they were shed from the Western Cordillera. At several places these Pleistocene deposits have been deformed as has been recognized by [17] already. Large-scale kink folds are visible along the road to San Jose de Quero (Figure 19) and an anticlinal hinge outcrops in a quarry near the

village of Ahuac. These folds suggest Quechua Phase deformation in the Central Highlands at least locally in sub-recent times.

5.4. Evolution of the Orogen

To place the deformation phases discussed above into a larger scale framework we compiled an orogenic timetable that includes the magmatic history, the stratigraphic sequences and the relative plate motions between the Nazca plate and the South American plate in Mesozoic and Cenozoic times. In the orogenic timetable shown in Figure 20, the Andes are divided into the structural domains used previously. The convergence rates and directions shown in Figure 20 are based on [20,21,100–102]. The magmatic history is taken from Figure 5 and the references mentioned in Section 3. We added the small plugs of Cenozoic age that are observed in the Central Highlands and the Eastern Cordillera. For simplicity we refrain from giving the names of the individual intrusions.

Figure 20. Orogenic timetable for the Central Andes of Peru. See text for discussion and references used for the compilation of convergence rates.
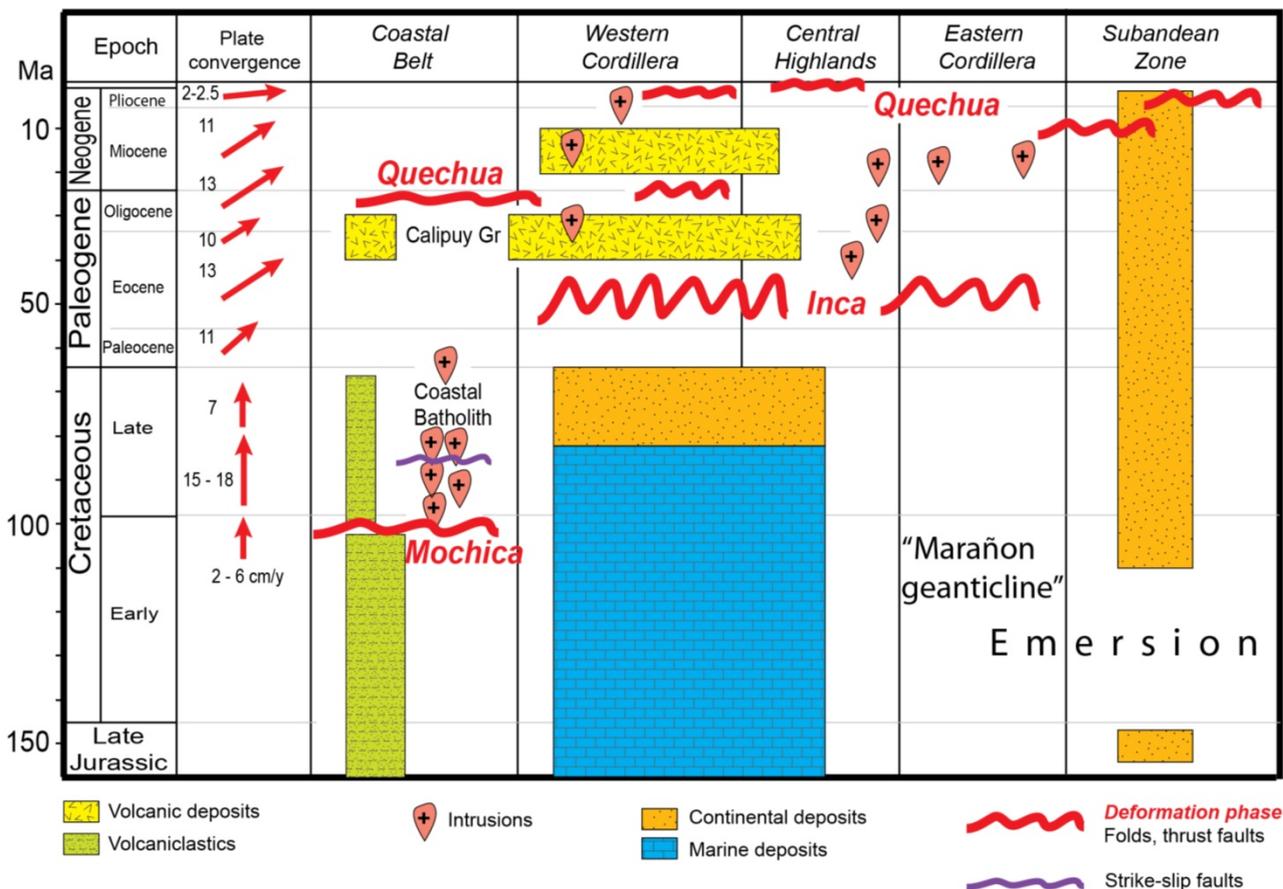
In the sedimentary sequences we only distinguish between marine and continental deposits; more details are given in Figure 4. Generally speaking, one recognizes the marine sedimentation restricted to the W-Peruvian trough and the lack of sedimentation within the Eastern Cordillera. This area has been referred to as the "Marañon geanticline" [17,91] that separated the marine domain from the continental deposits of the E-Peruvian basin in the Subandean Zone. Considering the spatial and temporal

distribution of the deformation phases within the Andes, it appears that the deformation front migrated eastward towards the Amazonas Craton. The late episodes of the Quechua Phase, however, affected some of the more internal parts of the Peruvian Andes, suggesting that in Late Neogene times the entire orogen was under compression.

Figure 20 also reveals that the temporal relationship between the deformation phases and the magmatic events. The emplacement of the Coastal Batholith occurred after the formation of the Mochica Phase folds it crosscut. This emplacement is coeval with strike-slip faulting as shown by [30]. The volcanic episode of the Eo-Oligocene Calipuy Group post-dates the Inca Phase. The unconformity at its base clearly indicates a phase of erosion between the Inca Phase deformation and the volcanic activity. The magmatic activity in Oligocene to Pliocene times is less ordered in space and time. Volcanic deposits are mainly restricted to the Western Cordillera, while intrusive complexes were emplaced throughout the Cordilleras and the Central Highlands. For the Cenozoic, a direct correlation between magmatic pulses and deformation phases seems fortuitous.

The plate convergence rates and directions changed considerably since Early Cretaceous. From Early Cretaceous on to the Paleocene, the convergence was oriented more or less N–S with a fast pulse (15–18 cm/year) in the early Late Cretaceous and a drop of the convergence rate to about 7 cm/year in the Late Cretaceous (see Figure 20). A change in convergence direction to NE–SW occurred in Paleocene times, with a fast pulses in the Eocene, between 55 and 40 Ma and between 25 and 10 Ma [102]. A more detailed discussion of the orogenic evolution in the framework of plate tectonics follows below.

Apart the purely temporal and spatial evolution of deformation in the orogen it is also of interest to see how the magnitude of deformation expressed in kilometers of shortening evolved. For the Mochica Phase shortening was restricted to the Coastal Area and amounts to 17–25 km (these and the following numbers correspond to the preferred values obtained from section balancing). In case of the Inca Phase shortening in the Western Cordillera, the Central Highlands and the Eastern Cordillera is roughly 75 km; 5 km stemming from the Raura–Viuda–San Juan de Quero fault system in the Western Cordillera, are subtracted and attributed to the Quechua Phase. Thus, shortening related to the Quechua Phase which apart this fault system includes the Subandean Zone and the eastern margin of the Eastern Cordillera, are estimated to be 30–47 km.

The time interval available for this shortening is *ca.* 10 Myr for the Mochica Phase, 20 Myr for the Inca Phase and 10 Myr for the Quechua Phase (precluding the gentle folding that occurred around the Oligocene–Miocene boundary). From these values an estimate for shortening rates can be obtained. These amount to roughly 2 mm/year for the Mochica Phase, 4 mm/year for the Inca Phase and 3–4.7 mm/year for the Quechua Phase. These shortening rates are less than the ones calculated for the Central Andes of Chile–Bolivia by [103] but are, with the exception of the Subandean Zone, of the same order of magnitude.

6. Discussion

The development of a structural model of the Peruvian Andes requires cross-sections that transect the entire orogen, are retro-deformable and display the correct local structural style. The sequence of deformation phases and their temporal relationship to magmatic events and angular unconformities observed in the field are synthesized to a model of the evolution of the Central Andes. This model is

then tested against the plate kinematic model involving mainly horizontal movements. Finally, the model of evolution is analyzed in terms of vertical movements that were responsible for building of a mountain chain.

6.1. Structural Style

The compression and shortening of the crust on a plate margin expresses itself in a variety of structurcal styles. In a thin-skinned tectonic style the cover sediments are stripped off their crystalline basement along a detachment horizon and shortened by folding and thrusting. Shortening in the crystalline basement rocks occurs independently at another locality. Examples include the Salt Range in Pakistan or the Jura Mountains [85]. In a basement involved thick-skinned style thrust faults cut into the crystalline basement but level off to form basement slabs that are some kilometers thick as is the case in the Alps or the Caledonides [85]. In a true thick-skinned tectonic style, the thrust faults dissect the entire crust and may even affect the Moho. Examples thereof include the Wind River Range in the U.S. or the Sierras Pampeanas in Argentina.

Mégard [17,18,91] reported on the structural style in the Central Andes of Peru. In his cross-sections he acknowledged the existence of a basal detachment in some instances, but continued the detachment faults down into the crystalline basement as steeply dipping reverse faults. Considering the important displacements along the observed thrust faults we think it unlikely that the detachment horizons steepen abruptly when entering the basement rocks. In other instances, the basement-cover contact is interpreted as being folded harmonically with the overlying sediments (op. cit.). This ductile behavior of basement rocks would require that they deformed at elevated temperatures. Our observations indicate low-temperature deformation, typical examples of which are displayed in Figure 21. Deformation in carbonates on fold limbs show evidence of multiple veining (Figure 21A) and pressure solution (Figure 21A–C). Oolithic limestones show no sign of pervasive millimeter-scale deformation (Figure 21B). In folds, individual beds retain their thickness but fold hinges are often accompanied by tectonic breccias (Figure 21D and E). We thus interpret the structures to depths of about 10 km to be more brittle in nature as is typical for low-temperature deformation.

The structural style within the Eastern Cordillera as presented in our cross-sections involving the existence of relatively steep reverse faults and folds differs from the style reported from the Eastern Cordillera in Bolivia [104–106]. There, the steep faults at the surface are linked to a shallow detachment at the base of the Early Paleozoic strata, which in turn is interpreted to involve 5–10 km thick flakes of crystalline basement nappes. While this basement involved thin-skinned style is thought to be E-vergent, the steep reverse faults at the surface point to a symmetric structure with a "backthrust belt" in the western part of the Eastern Cordillera [104]. In our study area, the Paleozoic sequence has largely been removed making a direct comparison difficult. However, the structures observed in Peru as shown in Figure 12 for example, point to a different style at the basement-cover contact as reported from Bolivia. We observe steeply dipping thrust faults cutting down into the crystalline basement in the core of the Eastern Cordillera.

In the Subandean Zone, the E-vergent imbricate thrusting with a shallow dipping detachment horizon described in Bolivia [104] compares to the structure in the Peruvian Andes as reported by [22,91] and shown in our Figure 14.

Figure 21. Deformation style at outcrop to hand-specimen scale. (**A**) Multiple veining in limestone of Pucará Group near Tarma (11°24.4' S, 75°49.1' W); (**B**) Jurassic olithic limestone near Tarma with oolites lacking any shape preferred orientation (11°27.3' S, 75°48.5' W); (**C**) Stylolites in limestones of Jumasha Formation near La Oroya (11°31.0' S, 75°55.25' W); (**D**) Brecciated limestone of the Chaucha Formaton in the core of an anticline (Saturn Anticline in Figure 10) SW of Huancayo (12°14.5' S, 75°38.3' W); (**E**) Brecciated carbonates of Pucará Group in the core of an anticline between Tarma and La Oroya (11°23.3' S, 75°51.1' W).
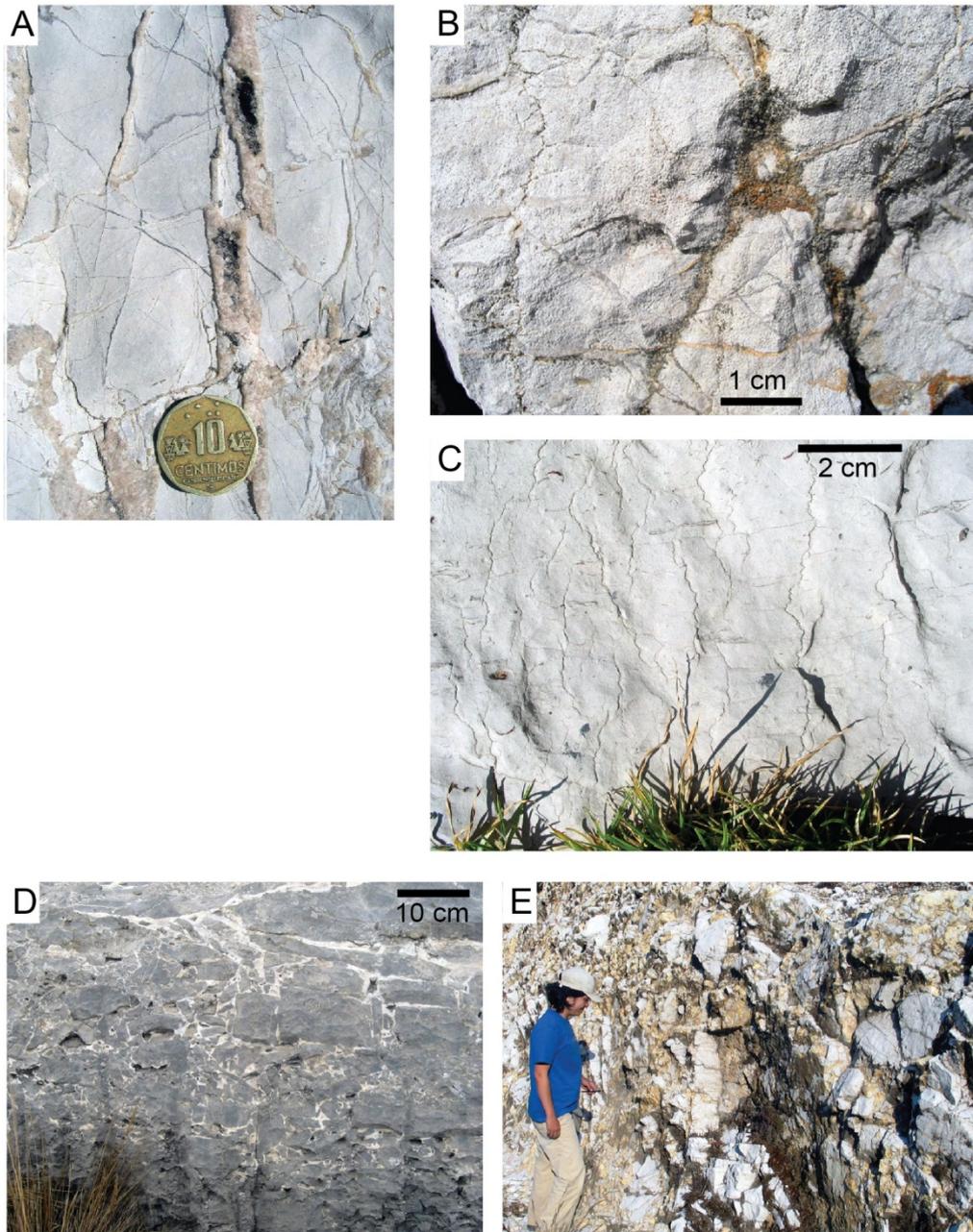
Shortening in the neighboring Bolivian Andes amounts to 150 km (42%) for the Eastern Cordillera and the Subandean Zone together [107], which must be compared to the 80 km (25%) obtained for the Southern Traverse (Figure 16) in the equivalent segment. [107] proposed that the higher shortening observed around the Bolivian orocline correlates with a thickened lithosphere. For the area farther to

the SE around the Bolivian orocline, [108] suggested a shortening of 123 km for the Subandean Zone combined with the Eastern Cordillera and concluded that in this segment of the Andes the Western Cordillera hidden beneath the Cenozoic volcanics must also have been shortened substantially and/or that crustal material had been added there in order to explain the thickness of the crust. Our analysis confirms extensive shortening in the Western Cordillera. In the cross-section shown in Figure 3, the South American crust restores to a length of 480 km if an original average crustal thickness of 35 km is assumed. This is slightly more than the retro-deformed lengths of 457 km of the Southern Traverse (Figure 16) taking the segment from the Subandean Zone to the Western Cordillera into account (and disregarding the 88 km of the Coastal Belt). But the detachment faults of the western part of the Western Cordillera do not directly feed into the crustal root, which is located farther to the northeast. We therefore speculate that at lower crustal level west-verging shearing moved lower crustal material from the tip of the crust into the crustal root. In Figure 3 this is schematically indicated by a single thrust fault in the subsurface of the Coastal Belt and Western Cordillera, although it is likely that the deformation at these depths is more ductile in nature. The removal of lower crust from the tip of the continental margin by tectonic erosion, its transfer to the northeast and its accretion to the upper plate by tectonic underplating could be caused by irregularities in the Nazca plate entering the subduction zone.

In the Western Cordillera we suspect a shallow dipping detachment between the Jurassic and the Cretaceous strata and a deeper one in the Triassic. Mégard modified his initial interpretation of 1978 [17] in 1987 [91] but retained the involvement of the crystalline basement by thrusting and folding. We prefer a solution whereby the cover is detached from the crystalline basement and where basement and cover then deform independently. Such a style has been documented in the Alps, the North American Cordillera and the Appalachians ([85] and references therein). The downward continuation of the thrust faults within the crystalline basement is neither exposed nor imaged by geophysical methods in the case of Peru. Judging from other orogens, where equivalent structures are exposed at the surface, such thrust faults are likely to be narrow fault zones in the upper crust and broaden into shear zones deeper down. Considering the extensive magmatism in the Andes, shear zones can be expected to broaden owing to thermal weakening of the crust. Ultimately, the crustal thickening as evident from the crustal root shown in Figure 3A may also be explained by the combined action of broadened shear zones. This is sustained by the fact that the thickened crust restores to the same length as the retro-deformed balanced cross-sections.

It has been argued by [109] that in the Central Andes crustal thickening was caused by magmatism in case of the Western Cordillera and by tectonic shortening in the Eastern Cordillera. For the Western Cordillera they argue that tectonic shortening was insignificant, a statement that is in stark contrast to our field observations in the Marañon fold-and-thrust belt. Some component of magmatic thickening is to be expected in the case of the Casma Volcanic Arc for which mantle-derived magmas are likely [55] and for the Coastal Batholith where partial melting in the mantle or in an underplated lower crust is assumed [66,67]. However, inspection of the cross-section in Figure 3 reveals that the thickest crust is located beneath the Western Cordillera and to the East of the two magmatic provinces with mantle derived melts. In fact, the magmatic rocks that crop out directly above the crustal root are the Cenozoic plutons for which a mantle source is not likely [70,72]. It thus seems that the crustal root is more likely to be the result of the tectonic shortening as discussed above in the context of the balanced sections. A similar conclusion was reached from a comparison of shortening obtained from balanced cross-sections in

the Bolivian orocline and the crustal thickness of the Altiplano area [108]. These authors argue that their preferred estimate of 123 km of shortening derived from the Subandean Zone and the Eastern Cordillera is not sufficient for explaining the crustal thickness needed for an Airy isostasy equilibrium. They mention three possibilities to explain the discrepancy: substantial shortening within the Western Cordillera (buried beneath the Paleogene volcanics in their study area), an initially thicker crust or magmatic underplating. Considering the shortening we report from the Western Cordillera in our study area, tectonic shortening would be sufficient to explain the crustal thickness beneath the Altiplano in the Bolivian orocline.

6.2. Deformation Phases in a Plate Kinematic Framework

The existence of mountain ranges at margins of continental plates strongly suggest a direct link between plate movements and the deformation of these margins. The deformation of plate margins leading to a mountain chain often represents a temporal sequence of deformation episodes. Since rate and directions of plate motions often change in the course of time it is of particular interest how they correlate with the deformation phases recognized in the upper plate.

A detailed discussion of the role of plate kinematic parameters in the Andean orogeny is given in [20,102]. We therefore highlight only the most important aspects here and concentrate on the Central Andes of Peru. As shown in Figure 20, the convergence between the Nazca and the South American plates in the Cretaceous was N–S oriented. The rapid increase from about 5 cm/year to about 15 cm/year at around 100 Ma correlates in time to the Mochica Phase, the following interval of high convergence rate in the early Late Cretaceous to the intrusion of the Coastal Batholith. Since the Casma Volcanic Arc sequence of the Coastal Belt was not affected by the Inca Phase deformation, the Mochica Phase likely represents the internal deformation of the volcanic arc sequence in the course of the accretion of the arc and the underlying Arequipa massif. As pointed out by [20], the intrusion of the Coastal Batholith occurred in the framework of a very oblique convergence and dextral strike slip movements [58]. Based on paleomagnetic data, however, the lateral motion of the Arequipa massif relative to the Amazonas craton seems to be minimal [15]. The drop in convergence rate to 7 cm/year in the Late Cretaceous (Campanian) is coeval to the change from marine to continental conditions in the W-Peruvian marginal basin (Western Cordillera–Central Highlands) [19]. Continental clastics were deposited in response to slower subsidence rates, a fact that can be explained by the effect of intraplate coupling. Numerical modeling of a frictional plate interface and variable trenchward upper plate motion suggests that as long that the South American plate was not moving sufficiently fast, friction along the plate interface tends to cause subsidence in the upper plate [110]. Consequently a drop in convergence rate can be held responsible for the drop in subsidence rate and overfilling of the W-Peruvian basin.

The change to a NE–SW oriented convergence direction in Paleocene times and the associated major change in the subduction geometry is attributed to a global plate kinematic reorganization in Late Paleocene–Eocene times [20]. The change in convergence direction is thought to have generated compressive stresses within the upper plate that initiated crustal thickening of the Central Andes and the onset of Inca Phase deformations. According to [102] the absolute plate velocity of the South American plate dropped from 5 to 3 cm/year at around 50 Ma. But the convergence rate between the

South American and Nazca plates itself was determined by the much faster moving Nazca plate and thus peaked at 55–40 Ma and 25–10 Ma. These time intervals correlate with the Inca and early episodes of the Quechua Phase deformations as discussed above. The interval of slower convergence in the Eo-Oligocene between 40 and 30 Ma covers the time interval of the volcanic event of the Calipuy Group and the erosional phase indicated by the angular unconformity at the base of these volcanics (the "Great unconformity" in Figure 18).

In an earlier paper based on a hotspot frame, [111] argued that the slowdown of the African plate by the collision with Eurasia lead to an accelerated westward motion of South America given that the spreading rate of the South Atlantic remained constant. The onset of this acceleration was interpreted to have occurred at around 30 Ma already. In any case, numerical modeling suggests that the trenchward migration of South America set the stage for crustal thickening, uplift and the formation of a mountain chain [110]. A fast pulse in plate convergence in the Oligo–Miocene, between 25 and 10 Ma [102] corresponds to episodes of Quechua Phase deformations. However, a more detailed correlation between convergence rates and individual episodes of Quechua Phase deformations is impossible to establish owing to the poor resolution of the timing available. The episodicity of Quechua Phase deformations is for example well documented in the Ayacucho area, where extensional or neutral episodes disrupted pulses of contraction in Miocene times [76]. Considering the local impact of the deformation episodes (see Figure 20), episodicity describes the nature of the evolution in time better than a protracted Quechua Phase deformation. This is corroborated by the more complete data set from the Central Andes of Chile–Bolivia [99], from where a rather complex temporal and spatial pattern is reported.

Farther North, in Ecuador, the Piñon terrane, an oceanic plateau with the Macuchi volcanic arc was accreted to the South American continent in latest Cretaceous and Paleocene times [112]. This accretion was responsible for the formation of the Western Cordillera of Ecuador. Whereas the Eastern Cordilleras of Ecuador and Peru possess a comparable structure, it is important to note that the Western Cordilleras of Ecuador and Peru are two entirely different mountain chains. In Peru, the Western Cordillera represents the compressed margin of the South American continent (including the Arequipa massif), whereas in Ecuador the Western Cordillera is made of rocks of the Macuchi volcanic arc of the Piñon terrane.

Considering the plate motion parameters, at least 2000 km of oceanic lithosphere was subducted beneath the South American plate in the segment of Peru since 20 Ma. This figure is in stark contrast to the comparably modest 120–150 km of shortening observed in the upper plate of this segment of the Andes. The accretionary wedge along the Central Andes of Peru incorporated roughly 25% only of the incoming sediment, the remainder was subducted [113]. However, this fraction varied considerably along strike owing to the oblique subduction of the Nazca Ridge [114]. Nevertheless, the sediment interlayer between the Nazca and South American plate could have caused a weak coupling which in turn would explain the modest amount of shortening observed in the upper plate.

6.3. Deformation Phases and Mountain Building

Three processes play a major rôle in mountain building: shortening by folding and thrusting that account for direct rock and surface uplift, buoyancy of the thickened crust carrying the weight of the

mountain chain and, finally, erosion which lowers the surface but triggers rock uplift by the effect of buoyancy. The effect of net erosion can be assessed by the degree of metamorphism observed in the rocks at the present surface. Compared to the Himalayas or the Alps the Andes experienced modest erosion despite the comparable high elevation of the mountain chain. In case of the Peruvian Andes intrusive complexes cropping out are generally of shallow nature indicating that only a few kilometers of rock were removed from their roofs. The sediments of the Western Cordillera and the Central Highlands show a slight or even no metamorphic overprint.

Crustal thickening by Inca and Quechua phase folding and thrusting was ultimately responsible for the formation of a mountain chain of high elevation. Two major Quechua Phase thrust systems were directly responsible for the creation of local relief. The Raura–Viuda–San Jose de Quero fault raised the Western Cordillera relative to the Central Highlands, and the thrust faults in the Subandean Zone next to the Eastern Cordillera raised the Eastern Cordillera to form summits up to 6000 m high. For the Altiplano of Chile and Bolivia, and thus the Central Highlands of Peru, (surface) uplift as determined from paleobotanical and landscape development occurred mainly in the past 10.7 Ma [115]. Apatite fission-track data reported from [116] suggest that exhumation commenced at 30 Ma in the Altiplano and the Eastern Cordillera of Bolivia, and at 10 Ma in the Subandean Zone. In southern Peru, (U-Th)/He data suggest the onset of uplift at 9 Ma [117], while geochronologic-stratigraphic analyses indicate an earlier onset at 13 Ma [118]. A young surface and rock uplift, finally, is also observed in the Andes of Ecuador where Miocene marine sediments deposited at 15–9 Ma are now at 3000 m above sea level [112,119].

Summing up we can conclude that the formation of the mountain chain is intimately related to Quechua Phase thrust faulting. Direct uplift (rock and surface uplift) occurred on WSW dipping thrust faults at the foot of the Western Cordillera (Raura–Viuda–San Juan de Quero fault system) and in the Subandean Zone including the foot of the Eastern Cordillera [7] and thus created the impressive relief. Thickening of the crust by these thrust faults and/or shear zones reaching deep into the thermally weakened crust sustained the uplifted mountain chain isostatically.

7. Conclusions

The structural style of the Central Andes of Peru varies between the individual cordilleras. It encompasses detachment folds above thrust faults that dip at a shallow angle towards the SW. Two balanced sections indicate a total shortening of 120–150 km across the entire orogen. Shortening rates can be estimated at 2–5 mm/year. Major thrust faults cut down into the crystalline basement and caused significant crustal shortening. The thickness of the crust can be explained by an original thickness of 35 km shortened by the same amount as determined from section balancing.

The Mesozoic–Cenozoic evolution of the Andes can be attributed to three major deformation phases. The earliest, the Mochica Phase is of Cretaceous age and corresponds to the amalgamation of the Casma Volcanic arc and the underlying Arequipa massif to the South American plate. Plate convergence was oblique and the accreted block was only moderately deformed in this process. The following Inca Phase resulted in a NE-vergent fold-and-thrust belt in the Western Cordillera, the Central Highlands and the Eastern Cordillera. It was likely triggered by a change to NE–SW plate convergence in the Eocene. The deformation front migrated farther to the NE in the Oligocene, such

that deformation of the third phase, the Quechua Phase, reached the Subandean Zone. Quechua Phase deformation affected the entire orogen from the Western Cordillera to the Subandean Zone, lasted until the Pliocene and is still active.

The Cenozoic compression of the western margin of South American plate caused not only crustal thickening but was responsible for the morphologic evolution of the Andes. Two major NE-vergent thrust systems attributed to the Quechua Phase were responsible for the higher elevations of the Western and the Eastern Cordilleras relative to the adjacent areas to the NE (Central Highlands and Subandean Zone).

Acknowledgments

Conflict of Interest

The authors declare no conflict of interest.

References

1. Barazangi, M.; Isacks, B.L. Spatial distribution of earthquakes and subduction of the Nazca plate beneath South America. *Geology* **1976**, *4*, 686–692.
2. Jordan, T.; Isacks, B.; Allmendiger, R.; Brewer, J.; Ramos, V.; Ando, C. Andean tectonics related to geometry of subducted Nazca plate. *Geol. Soc. Am. Bull.* **1983**, *94*, 341–361.
3. Ramos, V. Plate tectonic setting of the Andean Cordillera. *Episodes* **1999**, *22*, 183–190.
4. Suarez, G.; Gagnepain, J.; Cisternas, A.; Hatzfeld, D.; Molnar, P.; Ocola, L.; Roecker, S.W.; Viode, J.P. Tectonic deformation of the Andes and the configuration of the subducted slab in central Peru: Results from microseismic experiment. *Geophys. J. Int.* **1990**, *103*, 1–12.
5. Lindo, R.; Dorbath, C.; Cisternas, A.; Dorbath, L.; Ocola, L.; Morales, M. Subduction geometry in central Peru from a microseismicity survey: First results. *Tectonophysics* **1992**, *205*, 23–29.
6. Ramos, V.A.; Folguera, A. Andean Flat-Slab Subduction through Time. *Geol. Soc. Lond. Spec. Publ.* **2009**, *327*, 31–54.
7. Gonzalez, L.; Pfiffner, O.A. Morphologic evolution of the Central Andes of Peru. *Int. J. Earth Sci.* **2012**, *101*, 307–321.
8. Fukao, Y.; Yamamoto, A.; Kono, M. Gravity anomaly across the Peruvian Andes. *J. Geoph. Res. B* **1989**, *97*, 3867–3890.
9. Tassara, A.; Götze, H.-J.; Schmidt, S.; Hackney, R. Three-dimensional density model of the Nazca plate and the Andean continental margin. *J. Geoph. Res.* **2006**, *111*, B09404:1–B09404:26.

10. Cardona, A.; Cordani, U.G.; Ruiz, J.; Valencia, V.A.; Armstrong, R.; Chew, D.; Nutman, A.; Sanchez, A.W. U–Pb zircon geochronology and Nd isotopic signatures of the pre-mesozoic metamorphic basement of the Eastern Peruvian Andes: Growth and provenance of a Late Neoproterozoic to carboniferous accretionary orogen on the northewest margin of Gondwana. *J. Geol.* **2009**, *117*, 285–305.

11. Chew, D.; Schaltegger, U.; Miškovič, A.; Fontignie, D.; Frank, M. Deciphering the Tectonic Evolution of the Peruvian Segment of the Gondwana Margin. In *Géodynamique Andine: Résumés Étendus = Andean Geodynamics: Extended Abstracts = Geodinamica Andina: Resumenes Ampliados*; Institut de Recherche pour le Développement (IRD): Barcelona, Spain, 2005; pp. 166–169.

12. Chew, D.; Magna, T.; Kirkland, C.; Miškovič, A.; Cardona, A.; Schaltegger, U.; Spikings, R. Detrital zircon fingerprint of the Proto-Andes: Evidences for a Neoproterozoic active margin? *Precambrian Res.* **2008**, *167*, 186–200.

13. James, D.E.; Snoke, J.A. Structure and tectonics in the region of flat subduction beneath central Peru: Crust and uppermost mantle. *J. Geophys. Res. B* **1994**, *99*, 6899–6912.

14. Krabbenhöft, A.; Bialas, J.; Kopp, H.; Kukowski, N.; Hübscher, C. Crustal structure of the Peruvian continental margin from wide-angle seismic studies. *Geophys. J. Int.* **2004**, *159*, 749–764.

15. Shackelton, M.R.; Ries, A.C.; Coward, M.P.; Cobbold, P.R. Structure, metamorphism and geochronology of the Arequipa Massif of coastal Peru. *J. Geol. Soc. Lond.* **1979**, *136*, 195–214.

16. Steinmann, M. *Geologie von Peru* [in German]; Karl Winter Verlag: Heidelberg, Germany, 1929.

17. Mégard, F. *Etude Géologique des Andes du Pérou Central: Contribution à l'Étude Géologique des Andes No 1* [in French]; Mémoires 86; ORSTOM: Paris, France, 1978.

18. Mégard, F. The Andean orogenic period and its major structures in central and northern Peru. *J. Geol. Soc. Lond.* **1984**, *1*, 893–900.

19. Jaillard, E.; Soler, P. Cretaceous to Early Paleogene tectonic evolution of the northern Central Andes (0–18° S) and its relation to geodynamics. *Tectonophysics* **1996**, *259*, 47–53.

20. Jaillard, E.; Hérail, G.; Monfret, T.; Díaz-Martínez, E.; Baby, P.; Lavenu, A.; Dumont, J.F. Tectonic Evolution of the Andes of Ecuador, Peru, Bolivia and Northernmost Chile. In *Tectonic Evolution of South America*, Proceedings of 31st International Geological Congress, Rio de Janeiro, Brazil, 6–17 August 2000; Cordani, U.G., Milani, E.J., Thomaz, A., Campos, D.A., Eds.; FINEP; Fundo Setorial de Petróleo e Gás Natural: Rio de Janeiro, Brazil; pp. 481–559.

21. Soler, P.; Bonhomme, M.G. Relation of Magmatic Activìty to Plate Dynamics ìn Central Peru from Late Cretaceous to Present. In *Plutonism from Antarctica to Alaska*; Special Paper 241; Kay, S.M., Rapela, C.W., Eds.; Geological Society of America: Boulder, CO, USA, 1990; pp. 173–192.

22. Espurt, N.; Brusset, S.; Baby, P.; Hermoza, W.; Bolaños, R.; Uyen, D.; Déramond, J. Paleozoic structural controls on shortening transfer in the Subandean foreland thrust system, Ene and southern Ucayali basins, Peru. *Tectonics* **2008**, *27*, 1–21.

23. Gil, W.F. *Evolución Lateral de la Deformación de un Frente Orogénico: Ejemplo de las Cuencas Subandinas Entre 0° y 16°* [in Spanish]; Publicación Especial 4; Sociedad Geológica del Perú: Lima, Peru, 2002.

24. Carlier, G.; Gradin, G.; Laubacher, G.; Marocco, R.; Mégard, F. Present knowledge of the magmatic evolution of the eastern cordillera of Peru. *Earth Sci. Rev.* **1982**, *18*, 253–283.

25. Schaltegger, U.; Chew, D.; Miškovič, A. Neoproterozoic to Early Mesozoic Evolution of the Western Gondwana Margin: Evidence from the Eastern Cordillera of Peru. In Proceedings of XIII Congreso Peruano de Geología, Lima, Peru, 17–20 October 2006.

26. Wilson, J. Cretaceous stratigraphy of the central Andes of Peru. *AAPG Bull.* **1963**, *47*, 1–34.

27. Jacay, J.; Castillo, J.; Reátegui, T.; Pari, H. Carácterísticas sedimentológicas del Albiano (Grupo Casma)—Valle del Rio Chillon [in Spanish]. *Revista Inst. Investig. Fac. Geol. Minas Metal. Cienc. Geogr*. **2002**, *5*, 43–46.

28. Aleman, A.M. Stratigraphy, Sedimentology and Tectonic Evolution of the Rio Cañete Basin: Central Coastal Ranges of Peru. In Proceedings of the 3rd International Symposium of Andean Geodynamics (ISAG), St Malo, France, 17–19 September 1996; pp. 261–264.

29. Cobbing, E.J. The Tectonic Setting of the Peruvian Andes. In *Magmatism at a Plate Edge: The Peruvian Andes*; Pitcher, W.S., Atherton, M.P., Cobbing, E.J., Beckinsale, R., Eds.; Blackie and Son Ltd: Glasgow and London, UK; John Wiley and Sons: New York, NY, USA, 1985; pp. 3–12.

30. Polliand, M.; Schaltegger, U.; Frank, M.; Fontbotè, L. Formation of intra-arc volcano sedimentary basins in the western flank of the Peruvian Andes during Late Cretaceous oblique subduction: Field evidence and constrains from U–Pb ages and Hf isotopes. *Int. J. Earth Sci.* **2005**, *94*, 231–242.

31. Atherton, M.; Webb, S. Volcanic facies, structure and geochemistry of the marginal basin rocks of Central Peru. *J. South. Am. Earth Sci.* **1989**, *2*, 241–261.

32. Jacay, J.; Sempere, T. Emplacement Levels of the Coastal Batholith in Central Peru. In Proceedings of the 6th International Sympposium of Andean Geodynamics (ISAG), Barcelona, Spain, 12–14 September 2005; pp. 397–399.

33. Dalmayrac, B.; Laubacher, G.; Marocco, R.; Martínez, C.; Tomasi, P. La chaîne hercynienne d'amérique du sud: Structure et évolution d'un orogène intracratonique [in French]. *Geol. Rundsch.* **1971**, *69*, 1–21.

34. Mégard, F.; Caldas, J.; Paredes, J.; De la Cruz, N. *Geología de los Cuadrángulos de Tarma, La Oroya y Yauyos* [in Spanish]; Bolletin 69; Instituto Geológico Minero y Metalúrgico del Perú: Lima, Peru, 1996; Mapas: 23-l, 24-l, 25-l, Scale 1:100,000.

35. Scherrenberg, A.F.; Jacay, J.; Holcombe, R.J.; Rosenbaum, G. Stratigraphic variations across the Marañon Fold-Thrust Belt, Peru: Implications for the basin architecture of the West Peruvian Trough. *J. South. Am. Earth Sci.* **2012**, *38*, 147–158.

36. Szekely, T.; Grose, L.T. Stratigraphy of the Carbonate, Black Shale, and phosphate of the Pucará Group (Upper Triassic–Lower Jurassic), Central Andes, Peru. *Geol. Soc. Am. Bull*. **1972**, *83*, 407–428.

37. Rosas, S.; Fontboté, L.; Tankard, A. Tectonic evolution and paleogeography of the Mesozoic Pucará Basin, central Peru. *J. South. Am. Earth Sci*. **2007**, *24*, 1–24.

38. Rosas, S.; Fontboté, L. Sedimentology of the Cercapuquio and Chaucha Formations (Central Peru). In Proceedings of the International Sympposium of Andean Geodynamics (ISAG), Grenoble, France, 15–17 May 1990; pp. 15–17.

39. Moulin, N. Facies et Séquences des Dépôts de la Plate-Forme du Jurassique Moyen à l'Albien, et une Coupe Structurale des Andes du Pérou Central [in French]. Ph.D. Thesis, Université de Montpellier II, Montpellier, France, 1989.

40. Jaillard, E.; Arnaud-Vanneau, A. The Cenomanian-Turonian transition on the Peruvian margin. *Cretac. Res.* **1993**, *14*, 585–605.

41. Zapata, A.; Sanchez, A.; Carrasco, S.; Cardona, A.; Galdos, J.; Cerrón, F.; Sempere, T. The Lower Carboniferous of the Western Edge of Gondwana in Peru and Bolivia: Distribution of Sedimentary Basins and Associated Magmatism. In Proceedings of the 6th International Symposium of Andean Geodynamics (ISAG), Barcelona, Spain, 12–14 September 2005; pp. 817–820.

42. Díaz-Martínez, E. Estratigrafía y Paleogeografía del Paleozoico Superior del Norte de los Andes Centrales (Bolivia y sur del Perú) [in Spanish]. In *75 Aniversario Sociedad Geológica del Perú, Lima*; Macharé, J., Benavides, V., Rosas, S., Eds.; Sociedad Geológica del Perú: Lima, Peru, 1999; Volume 5, pp. 19–26.

43. Jacay, J.; Castillo, E.; Güimac, K. Sedimentary Evolution of Paleozoic Lithostratigraphic Units in Central Peru (Ambo-Huanuco Region). In Proceedings of the 4th European Meeting on the Palaeontology and Stratigraphy of Latin America, Madrid, Spain, 12–14 September 2007; *Cuadernos. del Museo Geominero*; Volume 8, pp. 219–221.

44. Newell, N.D.; Tafur, I. Ordovícico fosilífero en la Selva oriental del Perú [in Spanish]. *Bol. Soc. Geol. Perú.* **1943**, *14*, 5–16.

45. Jacay, J.; Sempere, T.; Carlier, G.; Carlotto, V. Late Paleozoic-Early Mesozoic Plutonism and Related Rifting in the Eastern Cordillera of Peru. In Proceedings of the 4th International Symposium of Andean Geodynamics (ISAG), Göttingen, Germany, 4–6 October 1999; pp. 350–362.

46. Miškovič, A.; Spikings, R.; Chew, D.M.; Košler, J.; Ulianov, A.; Schaltegger, U. Tectonomagmatic evolution of Eastern Amazonia: Geochemical characterization and zircon U–Pb geochronologic constraints from the Peruvian Eastern Cordillera granitoids. *Geol. Soc. Am. Bull.* **2009**, *121*, 1298–1324.

47. Mathalone, J.M.P.; Montoya, R.M. Petroleum Geology of the Sub Andean Basins of Peru. In *Petroleum Basins of South America*; Memoir 62l; Tankard, A.J., Suárez Soruco, R., Welsink, H.J., Eds.; American Association of Petroleum Geologists: Tulsa, OK, USA, 1995; pp. 423–444.

48. Kummel, B. Geological reconnaissance of the Contaman region Peru. *Geol. Soc. Am. Bull.* **1948**, *59*, 1217–1266.

49. Jacques, J.M. A tectonostratigraphic synthesis of the Sub-Andean basins: Implications for the geotectonic segmentation of the Andean Belt. *J. Geol. Soc. Lond.* **2003**, *160*, 687–701.

50. Hermoza, W.; Brusset, S.; Baby, P.; Gil, W.; Roddaz, M.; Guerrero, N.; Bolaños, M. The Huallaga foreland basin evolution: Thrust propagation in a deltaic enviroment, northen Peruvian Andes. *J. South. Am. Earth Sci.* **2005**, *19*, 21–34.

51. Pitcher, W.S. The anatomy of a batholith. *J. Geol. Soc. Lond.* **1978**, *135*, 157–182.

52. Pitcher, W.S.; Atherton, M.P.; Cobbing, E.J.; Beckinsale, R.D. *Magmatism at a Plate Edge: The Peruvian Andes*; Blackie and Son ltd: Glasgow and London, UK; John Wiley and Sons: New York, NY, USA, 1985.

53. Cobbing, E.J.; Pitcher, W.S.; Wilson, J.J.; Baldock, J.W.; Taylor, W.P.; McCourt, W.; Snelling, N.J. *The Geology of the Western Cordillera of Northern Peru*; Institute of Geological Sciences Overseas Memoir 5; Her Majesty's Stationery Office: Norwich, UK, 1981.

54. Chew, D.; Schaltegger, U.; Kosler, J.; Whitehouse, M.J.; Gutjahr, M.; Spikings, R.; Miškovič, A. U–Pb geochronologic evidence for the evolution of the Gondwana margin of the north-central Andes. *Geol. Soc. Am. Bull.* **2007**, *119*, 697–771.

55. Miškovič, A.; Schaltegger, U. Crustal growth along non-collisional cratonic margin: A Lu-Hf isotopic survey of the Eastern Cordillera granitoids of Peru. *Earth Planet. Sci. Lett.* **2009**, *279*, 303–315.

56. Lancelot, J.R.; Laubacher, G.; Marocco, R.; Reanud, U. U/Pb radiochronology of two granitic plutons from the eastern cordillera (Peru): Extent of Permian magmatic activity and consequences. *Geol. Rundsch.* **1978**, *67*, 236–243.

57. Soler, P.; Bonhomme, M.G.; Laubacher, G. Edades K-Ar de Rocas Intrusivas de la Región de Comas-Satipo (Cordillera oriental del Perú Central, implicaciones tectónicas) [in Spanish]. *Bol. Soc. Geol. Perú.* **1990**, *81*, 121–125.

58. Kontak, D.; Clark, A.; Farrar, E.; Strong, D. The Rift-Associated Permo-Triassic Magmatism of the Eastern Cordillera: A Precursor to the Andean Orogeny. In *Magmatism at a Plate Edge: The Peruvian Andes*; Pitcher, W.S., Atherton, M.P., Cobbing, E.J., Beckinsale, R.B., Eds.; Blackie and Son Ltd: Glasgow and London, UK; John Wiley and Sons: New York, NY, USA, 1985; pp. 3–12.

59. Atherton, M.P.; Sanderson, M.L.; Wander, V.; McCourt, W. The Volcanic Cover: Chemical Composition and the Origin of the Magmas of the Calipuy Group. In *Magmatism at a Plate Edge: The Peruvian Andes*; Pitcher, W.S., Atherton, M.P., Cobbing, E.J., Beckinsale, R., Eds.; Blackie and Son Ltd: Glasgow and London, UK; John Wiley and Sons: New York, NY, USA, 1985; pp. 273–284.

60. Mukasa, S.B.; Tilton, G.R. Zirkon U–Pb Ages of Super-Units in the Coastal Batholith, Peru. In *The Nature and Origin of Granite*; Pitcher, W.S., Ed.; Chapman and Hall: London, UK, 1985; pp. 203–207.

61. Mukasa, S.B. Zirkon U–Pb ages of super-units in the Coastal batholith, Peru: Implications for magmatic and tectonic processes. *Geol. Soc. Am. Bull.* **1986**, *97*, 241–254.

62. Bussell, M.A.; Pitcher, W.S. The Structural Controls of Batholith Emplacement. In *Magmatism at a Plate Edge: The Peruvian Andes*; Pitcher, W.S., Atherton, M.P., Cobbing, E.J., Beckinsale, R., Eds.; Blackie and Son Ltd: Glasgow and London, UK; John Wiley and Sons: New York, NY, USA, 1985; pp. 167–176.

63. Cobbing, E.J.; Pitcher, M.P. The Coastal Batholith of Central Peru. *J. Geol. Soc. Lond.* **1972**, *128*, 421–460.

64. Atherton, M.P.; Sanderson, M.L. The Chemical Variation and Evolution of the Super-Units of the Segmented Coastal Batholith. In *Magmatism at a Plate Edge: The Peruvian Andes*; Pitcher, M.P., Atherton, W.S., Cobbing, E.J., Beckinsale, R.B., Eds.; Blackie and Son Ltd: Glasgow and London, UK; John Wiley and Sons: New York, NY, USA, 1985; pp. 208–227.

65. Pitcher, W.S. Cordilleran-Type Batholiths: Magmatism and Crust Formation at a Plate Edge. In *The Nature and Origin of Granite*; Pitcher, W.S., Ed.; Chapman and Hall: London, UK, 1997; pp. 231–257.

66. McCourt, W.J. The geochemistry and petrography of the Coastal Batholith of Peru. *J. Geol. Soc. Lond.* **1981**, *138*, 407–420.

67. Mukasa, S.B. Common Pb isotopic composition of the Lima, Arequipa and Toquepala segments in the Coastal Batholith, Peru: Implications for magma genesis. *Geochim. Cosmochim. Acta* **1986**, *50*, 771–782.

68. Haederle, M.; Atherton, M.P. Shape and intrusion of the Coastal Batholith, Peru. *Tectonophysics* **2002**, *345*, 17–28.

69. Bissig, T.; Ullrich, T.; Tosdal, R.; Friedman, R.; Ebert, S. The time-space distribution of Eocene to Miocene magmatism in the central Peruvian polymetallic province and its metallogenetic implications. *J. South. Am. Earth Sci.* **2008**, *26*, 16–35.

70. Petford, N.; Atherton, M.P. Granitoid emplacement and deformation along a major crustal lineament: The Cordillera Blanca, Peru. *Tectonophysics* **1992**, *205*, 17–185.

71. Petford, N.; Atherton, M. Na-rich partial melts from newly underplated basaltic crust: The cordillera blanca batholith Peru. *J. Petrol.* **1996**, *37*, 1491–1521.

72. Petford, N.; Atherton, M.P.; Halliday, A.N. Rapid magma production rates, underplating and remelting in the Andes: Isotopic evidence from northern-central Peru (9°–11° S). *J. South. Am. Earth Sci.* **1996**, *9*, 69–78.

73. Farrar, E.; Noble, D.C. Timing of late Tertiary deformation in the Andes of Peru. *Geol. Soc. Am. Bull.* **1976**, *87*, 1247–1250.

74. Noble, D.C.; McKee, E.; Mégard, F. Early Tertiary "Incaic" tectnonism, uplift, and volcanic activity, Andes of Central Peru. *Geol. Soc. Am. Bull.* **1979**, *90*, 903–907.

75. McKee, E.H.; Noble, D.C. Miocene volcanism and deformation in the western Cordillera and high plateaus of south-central Peru. *Geol. Soc. Am. Bull.* **1982**, *93*, 657–662.

76. Wise, J.M.; Noble, D.C.; Zanetti, K.A.; Spell, T.L. Quechua II contraction in the Ayacucho intermontane basin: Evidence for rapid and episodic Neogene deformation in the Andes of central Perú. *J. South. Am. Earth Sci.* **2008**, *26*, 383–393.

77. Trumbull, R.B.; Riller, U.; Oncken, O.; Scheuber, E.; Munier, K.; Hongn, F. The Time-Space Distribution of Cenozoic Volcanism in the South-Central Andes: A New Data Compilation and Some Tectonic Implications. In *The Andes–Active Subduction Orogeny*; Frontiers in Earth Sciences Series 1; Oncken, O., Chong, G., Franz, G., Götze, H.-J., Ramos, V.A., Strecker, M.R., Wigger, P., Eds.; Springer: Berlin, Germany, 2006; pp. 29–44.

78. Angeles, C. Le chevauchements de la Cordillère Occidentala par 12°15' S (Andes du Péru Central) [in French]. Ph.D. thesis, Universite de Montpellier II, Montpellier, France, 1987.

79. Sempere, T.; Jacay, J.; Carlotto, V.; Martinez, W.; Bedoya, C.; Fornari, M.; Roperch, P.; Acosta, H.; Acosta, J.; Cerpa, L.; *et al.* Sistemas Transcurrentes de Escala Litosférica en el sur del Perú [in Spanish]. In *Nuevas Contribuciones del IRD y sus Contrapartes al Conocimiento Geológico del sur del Perú*; Publicación Especial 5; Jacay, J., Sempere, T., Eds.; Sociedad Geológica del Perú: Lima, Peru, 2004; pp. 105–110.

80. Jacay, J. Análisis de la Sedimentación del Sistema Cretáceo de los Andes del Perú Central [in Spanish]. *Revista Inst. Investig. Fac. Geol. Minas Metal. Cienc. Geogr.* **2005**, *8*, 49–59.

81. Mégard, F.; Dalmayrac, B.; Laubacher, G.; Marocco, R.; Martinez, C.; Paredes, J.; Tomasi, P. La Chaine Hercynienne au Pérou et en Bolivie, premiers résultats [in French]. *Cah. Orstom Sér. Géol.* **1971**, *3*, 5–44.

82. Dorbath, C.; Dorbath, L.; Cisternas, A.; Deverchère, J.; Sebrier, M. Seismicity of the Huancayo Basin (Central Peru) and the Huaytapallana Fault. *J. South. Am. Earth Sci.* **1990**, *3*, 21–29.

83. Dorbath, L.; Dorbath, C.; Jimenez, E.; Rivera, L. Seismicity and tectonic deformation in the Eastern Cordillera and the sub-Andean zone of central Peru. *J. South. Am. Earth Sci.* **1991**, *4*, 13–24.

84. Soler, P.; Rotach-Toulhoat, N. Sr-Nd isotope compositions of cenozoic granitoids along a traverse of the central Peruvian Andes. *Geol. J.* **1990**, *25*, 351–358.

85. Pfiffner, O.A. Thick-Skinned and Thin-Skinned Styles of Continental Contraction. In *Styles of Continental Contraction*; Special Paper 414; Mazzoli, S., Butler, R.W.H., Eds.; Geological Society of America*:* Boulder, CO, USA, 2006; pp. 153–177.

86. Dahlstrom, C.D.A. Balanced cross sections. *Can. J. Earth Sci.* **1969**, *6*, 743–757.

87. Boyer, S.; Elliot, D. Thrust Systems. *AAPG Bull.* **1982**, *66*, 1196–1230.

88. Dahlstrom, C.D.A. Geometric constrains derived from the law of conservation of volume and applied to evolutionary models for detachment folding. *AAPG Bull.* **1990**, *74*, 336–344.

89. Jamison, W.R. Geometric analysis of fold development in overthrust terranes. *J. Struct. Geol.* **1987**, *9*, 207–219.

90. Pfiffner, O.A. Displacements along thrust faults. *Eclogae Geologicae Helvetiae* **1985**, *78*, 313–333.

91. Mégard, F. Structure and Evolution of the Peruvian Andes. In *The Anatomy of Mountain Ranges*; Schaer, J.-P., Rodgers, J., Eds.; Princeton University Press: Princeton, NJ, USA, 1987; pp. 179–210.

92. Laubacher, G.; Naeser, W. Fission-track dating of granitic rocks from the Eastern Cordillera of Peru: Evidence for Late Jurassic and Cenozoic cooling. *J. Geol. Soc. Lond.* **1994**, *151*, 473–483.

93. Sandeman, H.; Clark, A.; Farrar, E. An Integrated Tectono-Magmatic Model for the evolution of the Southern Peruvian Andes (13°–20°) since 55 Ma. *Int. Geol. Rev.* **1995**, *37*, 1039–1073.

94. McNulty, B.; Farber, F. Active detachment faulting above the Peruvian flat slab. *Geology* **2002**, *30*, 567–570.

95. Berger, A.; Rosenberg, C.; Schmid, S.M. Ascent, emplacement and exhumation of the Bergell pluton within the Southern Steep Belt of the Central Alps. *Schweiz. Mineral. Petrogr. Mitt.* **1996**, *76*, 357–382.

96. Dalmayrac, B.; Molnar, P. Parallel thrust and normal faulting in Peru and constraints on the state of stress. *Earth Planet. Sci. Lett.* **1981**, *55*, 473–481.

97. Schwartz, D.P. Paleoseismicity and neotectonics of the Cordillera Blanca fault zone, northern Peruvian Andes. *J. Geophys. Res. B.* **1988**, *93*, 4712–4730.

98. Allmendinger, R.W.; Smalley, R., Jr; Bevis, M.; Caprio, H.; Brooks, B. Bending the Bolivian orocline in real time. *Geology* **2005**, *33*, 905–908.

99. Oncken, O.; Hindle, D.; Kley, J.; Elger, K.; Victor, P.; Schemmann, K. Deformation of the Andean Upper Plate System–Facts, Fiction, and Constraints for Modellers. In *The Andes–Active Subduction Orogeny*; Frontiers in Earth Sciences Series 1; Oncken, O., Chong, G., Franz, G., Götze, H.-J., Ramos, V.A., Strecker, M.R., Wigger, P., Eds.; Springer: Berlin, Germany, 2006; pp. 3–28.

100. Pilger, R. Plate reconstruction, aseismic ridges, and low-angle subduction beneath the Andes. *Geol. Soc. Am. Bull.* **1981**. *92*, 448–456.

101. Pardo-Casas, F.; Molnar, P. Relative motion of the Nazca (Farallon) and South American Plates since Late Cretaceous time. *Tectonics* **1987**, *6*, 233–248.

102. Sdrolias, M.; Müller, R.D. Controls on back-arc basin formation. *Geochem. Geophys. Geosyst.* **2006**, *7*, Q04016:1–Q04016:40.

103. Oncken, O.; Boutelier, D.; Dresen, G.; Schemmann, K. Strain accumulation controls failure of a plate boundary zone: Linking deformations of the Central Andes and lithosphere mechanics. *Geochem. Geophys. Geosyst.* **2012**, *13*, Q12007:1–Q12007:22.

104. Kley, J. Geologic and geometric constraints on a kinematic model of the Bolivian orocline. *J. South. Am. Earth Sci.* **1999**, *12*, 221–235.

105. McQuarry, N.; DeCelles, P.G. Geometry and structural evolution of the central Andean backthrust belt, Bolivia. *Tectonics* **2001**, *20*, 669–692.

106. McQuarry, N.; Davis, G.H. Crossing the several scales of strain-accomplishing mechanisms in the hinterland of the central Andean fold-thrust belt, Bolivia. *J. Struct. Geol.* **2002**, *24*, 1587–1602.

107. Kley, J.; Monaldi, C.R.; Salfity, J.A. Along-strike segmentation of the Andean foreland: Causes and consequences. *Tectonophysics* **1999**, *301*, 75–94.

108. Gotberg, N.; McQuarrie, N.; Caillaux, V.C. Comparison of crustal thickening budget and shortening estimates in southern Peru (12°–14° S): Implications for mass balance and rotations in the "Bolivian orocline". *Geol. Soc. Am. Bull.* **2010**, *122*, 727–742.

109. Sempere, T.; Jacay, J. Anatomy of the Central Andes: Distinguishing between Western, Magmatic Andes and Eastern, Tectonic Andes. In Proceedings of the 7th International Symposium of Andean Geodynamics (ISAG), Nice, France, 2–4 September 2008; pp. 505–507.

110. Hampel, A.; Pfiffner, A. Relative Importance of Trenchward Upper Plate Motion and Friction along the Plate Interface for the Topographic Evolution of Mountain Belts. In *Analogue and Numerical Modelling of Crustal-Scale Processes*; Special Publication 253; Buiter, S.J.H., Schreurs, G., Eds.; The Geological Society: London, UK, 2006; pp. 105–115.

111. Silver, P.; Russo, R.; Lithgow-Bertelloni, C. Coupling of the south American and African plate motion and plate deformation. *Science* **1998**, *129*, 60–63.

112. Ramos, V.A.; Aleman, A. Tectonic Evolution of the Andes. In *Tectonic Evolution of South America*, Proceedings of 31st International Geological Congress, Rio de Janeiro, Brazil, 6–17 August 2000; Cordani, U.G., Milani, E.J., Thomaz, A., Campos, D.A., Eds.; FINEP; Fundo Setorial de Petróleo e Gás Natural: Rio de Janeiro, Brazil; pp. 635–685.

113. Von Huene, R.; Scholl, D.W. Observations at convergent margins concerning sediment subduction, subduction erosion, and the growth of continental crust. *Rev. Geophys.* **1991**, *29*, 279–316.

114. Von Huene, R.; Pecher, I.A.; Gutscher, M.-A. Development of the accretionary prism along Peru and material flux after subduction of the Nazca Ridge. *Tectonics* **1996**, *15*, 19–33.

115. Gregory-Wodzicki, K.M. Uplift history of the Central Northern Andes: A review. *Geol. Soc. Am. Bull.* **2000**, *112*, 1092–1105.

116. Ege, H.; Sobel, E.R.; Scheuber, E.; Jacobshagen, V. Exhumation history of the southern Altiplano plateau (southern Bolivia) constrained by apatite fission track thermochronology. *Tectonics* **2007**, *26*, TC1004:1–TC1004:24.

117. Schildgren, T.F.; Hodges, K.V.; Whipple, K.X.; Reiers, P.W.; Pringle, M.S. Uplift of the western margin of the Andean plateau revealed from canyon incision, southern Peru. *Geology* **2007**, *35*, 523–526.

118. Thouret, J.C.; Wörner, G.; Gunnell, Y.; Singer, B.; Zahn, X.; Souriot, T. Geochronologic and stratigraphic constrains on canyon incision and Miocene uplift of the Central Andes in Peru. *Earth Planet. Sci. Lett.* **2007**, *263*, 151–166.

119. Steinmann, M.; Hungerbühler, D.; Seward, D.; Winkler, W. Neogene tectonic evolution and exhumation of the southern Ecuadorian Andes: A combined stratigraphy and fission-track approach. *Tectonophys* **1999**, *307*, 255–276.